Politecnico di Torino

Politecnico di Torino

Corso di Laurea

A.a. 2024/2025

Graduation Session 16th October 2025

Sodium-ion Batteries Anode Life Cycle Inventory Compilation and Literature Meta-Analysis

Supervisors:

Dr. Giovanni Andrea Blengini, Polito

Dr. Silvia Bodoardo, Polito

Luka Smajila, KTH

Candidate:

Pradhyumna Danda Ravindra Kumar

Acknowledgements

This thesis work has been carried out as part of a larger project on the sustainability assessment of sodium-ion batteries for energy storage applications.

I want to express my sincere gratitude to my thesis advisor, Luka Smajila at KTH, who introduced me to this project and provided continuous support, guidance, and valuable feedback throughout the entire process.

I am also very grateful to my supervisors at Politecnico di Torino, Dr. Giovanni Andrea Blengini and Dr. Silvia Bodoardo, for their encouragement, insights, and advice, which have helped me during the thesis. A special thanks to Guilia Pezzin for her guidance and for always being available to discuss and support me during this work.

I am thankful as well to my colleagues Aditya, Renga Preethi, Sharada, and Tang, with whom I shared this project. Although we worked on different work packages, we constantly supported and motivated each other during the semester.

Finally, I would like to thank all my classmates and everyone who has supported me in any way during this journey.

Stockholm, 16th September 2025
Pradhyumna Danda Ravindra Kumar

Table of Contents

List of Tables

List of Figures

Glossary

ADP

Abiotic Depletion Potential

CAGR

Compound Annual Growth Rate

CEI

Cathode Electrolyte Interphase

CNF

Carbon Nanofiber

CRP

Commercial Red Phosphorus

CTAB

Cetyltrimethylammonium Bromide

DMF

N,N-Dimethylformamide

DME

Dimethoxyethane

GWP

Global Warming Potential

HC

Hard Carbon

HF

Hydrofluoric Acid

HTC

Hydrothermal Carbonisation

ICE

Initial Coulombic Efficiency

ILCD

International Reference Life Cycle Data

LCA

Life Cycle Assessment

LCI

Life Cycle Inventory

LCIA

Life Cycle Impact Assessment

LIBs

Lithium-Ion Batteries

MJ

Megajoule (energy unit)

MXene

Transition metal carbides/nitrides (e.g., $Ti_3C_2T_x$)

PAN

Polyacrylonitrile

PVP

Polyvinylpyrrolidone

rGO

Reduced Graphene Oxide

ReCiPe

Harmonized Life Cycle Impact Assessment method

SEI

Solid Electrolyte Interphase

SIBs

Sodium-Ion Batteries

TEOS

Tetraethyl Orthosilicate

Wh/kg

Watt-hour per kilogram (specific energy)

kWh

Kilowatt-hour (energy unit)

Chapter 1

Introduction

1.1 Background

The shift in the global energy trend towards renewable energy and electrification of multiple sectors has intensified the demand for efficient, scalable, and environmentally responsible energy storage systems[1][2][3]. Batteries are really at the core of the changes we are seeing in energy today. They play a crucial role in making renewable energy sources work together, help us create more decentralised power systems, and drive the shift towards electric transportation[4]. For over thirty years, lithium-ion batteries (LIBs) have led the way in this journey, due to their impressive energy efficiency and dependable performance. However, the success of LIBs has brought new challenges[5].

Lithium is a scarce element which is predominantly concentrated in production areas of South America and Australia, being most prominent[6]. Lithium production requires high-energy and water inputs, and it tends to occur in environmentally sensitive areas, raising concerns about environmental degradation and socioeconomic conflicts[7]. Apart from lithium, the supply chain of other critical LIB ingredients, such as cobalt, is also associated with other sustainability concerns[8]. These intertwined challenges raise valid questions about the scalability and ethical feasibility of lithium-ion battery technologies as the foundation for future global electrification.

Amid these difficulties, sodium-ion batteries (SIBs) have emerged as a compelling alternative. Sodium is the sixth most abundant element in the environment, and can even be economically recovered from seawater[9]. Unlike lithium, sodium is not classified as a critical raw material and is not subject to the same geographical or geopolitical supply constraints[10]. Although current SIBs tend to display lower theoretical energy densities than their lithium-ion counterparts, their material

abundance, lower cost, and improved sustainability make them especially promising for stationary grid storage and other mass-market energy uses where weight is less critical[11]. For these applications, resource security and lifetime cost can outweigh moderate compromises in volumetric or gravimetric energy density.

Recent studies in SIBs, particularly cathode, anode, and electrolyte design, have brought these technologies to the verge of large-scale commercialisation[10][2]. Business giants CATL and Faradion have announced the use of prototype SIB cells in stationary storage applications, which indicates robust development towards practical applications. These developments highlight the need to integrate systemic sustainability assessments into the advancement and upscaling of alternative battery chemistries, so that technological potential is weighed against real, sustainable environmental benefits[12][13].

1.2 Importance of Anode Materials in Sodium-Ion Batteries

Sodium-ion battery (SIB) performance is characterised by the electrochemical properties of anode and cathode materials. Although cathode design has often been in focus due to its influence on nominal cell voltage and accessible capacity, anode material characterises equally significant functionality[14][15].

Anode material in SIBs has an impact on a range of significant performance parameters:

- Reversible capacity and energy density: The capacity of the anode to accommodate sodium defines the total cell storage energy, where the carbon-type and alloy-type anodes store sodium in different ways[15].
- Working voltage and efficiency: The electrochemical potential of the anode relative to sodium metal defines the total output voltage and energy efficiency of the battery.
- Cycle stability and safety: Anode structural stability, resistance to volume expansion, and suppression of undesirable side reactions determine the safety of operation and the cycle lifespan.
- Cost and sustainability: Synthesis energy consumption, processing complexity, and raw material needs play immense roles in SIB economic and environmental costs[16].

Hard carbon remains the benchmark SIB anode material to date, valued for moderate capacity, high cycling stability, and precursor availability. Nonetheless, hard carbon anodes show poor initial Coulombic efficiency and need high-temperature pyrolysis, which is energy-intensive and costly. Alloy-type anodes, made from tin, antimony, or phosphorus, can provide significantly higher theoretical capacities due to the potential for Na-rich alloy formation; however, they suffer from high volume change during cycling, resulting in rapid capacity loss and mechanical distortion. Transition metal oxides and sulfides, as well as high-performance carbon-based nanostructures, also present pathways to higher capacity, but often with greater environmental consequences, notably through the adoption of energy-intensive synthesis methods or toxic precursors[16][17][18][19][20].

The environmental effects of many anode materials are severe. High-temperature calcination, extensive use of solvents (e.g., N,N-dimethylformamide), and the use of precursors such as red phosphorus or antimony oxide can lead to severe resource utilisation and toxicity problems. For some SIB chemistries, the environmental burden associated with anode production may be as much as, or even more than, that of cathode synthesis; consequently, anode selection becomes not only critical to maximise electrochemistry but also to render sodium-ion battery technology sustainable overall[17][21][22].

1.3 Research Gap

While more attention has recently been given to sodium-ion technology, by far the majority of the published sustainability research until now has been cathode-focused or substantially based on lithium-ion battery (LIB) data[23]. The majority of life cycle assessment (LCA) studies for sodium-ion batteries (SIBs) currently available either allocate the anode as model carbon or use proxy data sets with no resemblance to the synthesis conditions or precursors reported in the literature[24].

There are several recent reviews describing the electrochemical properties of different anode classes in SIBs, but not quantifying environmental effects or compiling standardised life cycle inventories[25][26]. For instance, the 2025 Royal Society of Chemistry review of ball-milling synthesis routes does not mention process design optimisation but lacks standard inventory data that can be applied for LCA[25]. Therefore, data on the environmental effects of producing possible anode materials, such as phosphorus composites, antimony oxides, and graphene-based nanostructures, is dispersed, inconsistent, and difficult to compare across research[17].

This data shortfall is necessary. Without consolidated and standardised life cycle inventory (LCI) data, upcoming LCAs for sodium-ion batteries can provide incomplete or inaccurate results[24]. Researchers and policymakers are hindered from comparing trade-offs among various anode chemistries or process "hotspots" that disproportionately contribute to environmental concerns[17]. Industry players also lack readily available data upon which to base decisions on whether commercial-scale commercialisation of new anode technologies is environmentally justified[27].

1.4 Objectives and Scopes

This thesis addresses the above research gap by developing a comprehensive life cycle inventory (LCI) database for nine prominent sodium-ion battery anode active materials. Building on a systematic meta-analysis of the scientific literature, the work compiles synthesis routes, precursor requirements, and processing energy into standardized gram-based inventories that can be mapped onto existing LCI databases such as ecoinvent.
The objectives of this thesis are therefore:

- To conduct a meta-analysis of published studies on the synthesis of sodium-ion battery anode active materials, extracting consistent data on inputs, energy use, yields, and by-products.
- To identify hotspots and gaps in terms of environmental burden, resource depletion potential, and data availability, thereby informing both future LCA studies and research directions in sodium-ion battery development.

The scope of this thesis is limited to covering the production of anode active materials only. Downstream processes such as electrode fabrication, full-cell assembly, and end-of-life recycling are beyond the scope of this work, as they are better addressed in holistic battery-level analysis. Similarly, this work focuses exclusively on sodium-ion battery chemistries and does not attempt to make detailed comparisons with lithium-ion systems.

By developing the consolidated LCI database for a various sodium-ion anode active materials, this thesis contributes to closing a gap in the sustainability assessment of emerging energy storage technologies. The results are intended to serve as a foundation for future life cycle assessments, enabling researchers, industry, and policymakers to make more informed decisions about the trade-offs and prospects of sodium-ion batteries in the global energy transition.

Chapter 2

Literature Review

2.1 Overview of Sodium-Ion Batteries

2.1.1 Operating Principles

Sodium-ion batteries (SIBs) are rechargeable electrochemical energy storage devices involving the reversible intercalation of sodium ions (Na^+) into electrode materials, fundamentally equivalent to lithium-ion technology but using earth-abundant sodium resources[28]. The electrochemical principle is the shuttling of sodium ions in an electrolyte medium between cathode and anode materials while electrons are transferred through an outside circuit to maintain charge balance[29]. Upon discharge, the ions of sodium flow from the anode to the cathode through the electrolyte as electrons flow around the outside circuit to generate electricity to supply devices[30]. Discharging is the reverse of the process where external electrical energy drives the ions of sodium back to the anode and stores chemical energy in the electrode structures. A representation of charge transfer in sodium-ion batteries is shown in the Figure 2.1.

The redox chemistry is during charging cathode oxidises, when sodium ions are removed and released into the electrolyte, and anode reduction, where the ions are intercalated or stored. The cell voltage is determined by the electrochemical potential difference between electrode materials, typically ranging between 2.5 and 3.7 V.

2.1.2 Components and Functionality

The architectural functionality of sodium-ion batteries has different crucial components enabling the electrochemical conversion of energy. The cathode provides the sodium ions within the initially discharged cell state, which are composed of intercalated sodium ions that are reversibly extracted under charging conditions.

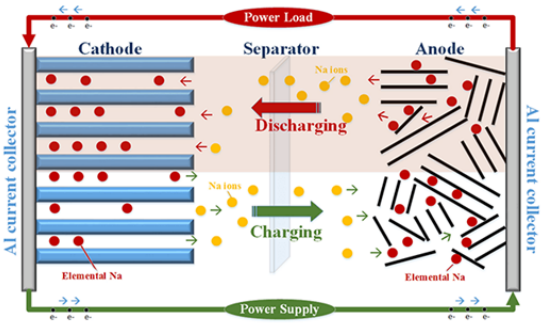

Figure 2.1: Sodium ion battery working principle [31]

During operation, the cathode undergoes processes of oxidation, where sodium ions are emitted into the electrolyte and concurrently receive electrons from the external circuit. The specific electrochemical behaviour depends on the crystal structure of the host material and the sodium diffusion channels[32].

The anode is the storage reservoir for sodium ions, initially free from sodium ions in the discharged state. During the charging process, it accommodates the incoming sodium ions through intercalation, alloying, or conversion-type processes. The anode material must provide sufficient sodium storage capacity with structural stability to prevent capacity loss caused by volume expansion or side reactions[28].

The electrolyte conducts sodium ions between electrodes, yet it is electronically insulating. It is typically designed by dissolving sodium salts in organic solvents containing carbonates, which enables ionic conductance and forms protective interphase layers at electrode surfaces. Critical to battery operation is the formation of solid-electrolyte interphase (SEI) layers on the anode and cathode-electrolyte interphase (CEI) layers on the cathode that prevent incessant electrolyte decomposition and enable stable cycling performance[28].

The separator provides physical separation of electrodes by ionic transport with safety through the avoidance of internal short circuits with low ionic resistance for effective battery operation[29]. Current collectors, typically aluminium and copper foil, enable electronic conductivity and mechanical support for the active material while enabling effective charge collection upon operation[24].

2.1.3 Current Commercialisation Status

Sodium-ion battery technology has evolved from laboratory development to its first commercial use, with 2025 marking a milestone in transitioning to industrial-scale production[33]. The global sodium-ion battery market is expected to grow from USD 307.4 million in 2025 to USD 2,932 million by 2035, at a compound annual growth rate (CAGR) of 25.3%, indicating robust commercial traction[34].

CATL has achieved commercial milestones with second-generation sodium-ion batteries at 200 Wh/kg energy density and operational capability at -40°C, with mass production already underway for late 2025[33][35]. HiNa Battery Technology demonstrated commercial achievement with the world's first 100 MWh sodium-ion energy storage project and built manufacturing capabilities in multiple cell formats, including cylindrical, prismatic, and blade shapes[33].

Current commercial applications are centered in stationary energy storage and grid-scale integration of renewable sources, where cost advantages due to sodium-ion technology relative to energy density limitations are balanced over lithium-ion technology. Use in the electric automobile industry is currently limited to small-sized automobiles in China's A00-class segment by virtue of available sodium-ion technology energy density levels, at 160-165 Wh/kg[36].

The capacity for production is rapidly growing, with currently only a few hundred gigawatt-hours (GWh) of yearly capacity, but large-scale future growth is in the pipeline as manufacturers prepare for greater market penetration[37]. The technology is expected to achieve cost parity with lithium iron phosphate batteries in the late 2020s, thanks to material cost advantages, where sodium is available at approximately $0.05 per kilogram, compared with lithium at $15 per kilogram. Support from governments, such as that of the U.S. Department of Energy's $50 million LENS consortium, is supporting in technological progress and commercial deployment to reduce reliance on lithium supply chains and enhance energy storage sustainability[33].

2.2 Anode Materials for Sodium-Ion Batteries

2.2.1 Importance of Anode Selection in Sodium-Ion Batteries

For sodium-ion battery (SIB) systems, the anode material determines fundamentally critical performance attributes such as working voltage, reversible capacity, rate capability, initial coulombic efficiency (ICE), and long-term cycling stability. Unlike

for lithium-ion batteries where stage-I intercalation (LiC_6) graphite has been the default anode material, SIBs have yet to converge on a standard anode material. This deviation is primarily caused by the larger ionic radius of Na^+ (1.07 Å) compared to Li^+ (0.76 Å), which discourages good graphite intercalation and creates kinetic impediments through reduced diffusion kinetics and increased structural stress during cycling. The absence of a single "default" anode maintains the SIB anode space pluralistic and competitive, presenting opportunities and challenges for technology innovation and sustainability tuning[38][39][40].

2.2.2 Mechanistic Classification Framework

Contemporary research categorises SIB anode materials based on their intrinsic sodium storage mechanisms as showin in the Figure 2.2, which share distinguishing electrochemical characteristics as well as sustainability issues[38]:

- Intercalation/Insertion Mechanisms allow Na^+ insertion into host lattices with minimal structural disturbance, typically resulting in small volume changes (<10%) and higher structural stability during long-term cycling. Examples include hard carbons, soft carbons, certain polyanionic hosts, and MXenes[41][40].
- Conversion Mechanisms consist of Na^+ reactions that form new phases with high theoretical capacities (400-1000 mAh g^{-1}) but are associated with high volume expansion (>100%) and resistive product growth. Transition-metal oxides, sulfides, and phosphides are the best first-charge primary examples[42].
- Alloying Mechanisms consist of the formation of Na-metal alloys, offering excellent theoretical capacities (400-2590 mAh g^{-1}) but inducing unacceptable volumetric expansion (>200%) that causes extreme mechanical instability and pulverisation pressures[43][44][45].

2.2.3 Intercalation/Insertion Anodes

Hard Carbon Materials are the technologically most sophisticated SIB anode replacement, functioning through a double-mechanism mechanism: Na^+ adsorption at defective sites and intercalation into disordered graphene planes in the sloping region (2.0 to 0.15 V), supplemented by micropore filling in the low-voltage plateau region (approx. 0.1 V). Current hard carbon anodes achieve reversible capacities of 200 to 350 $mAhg^{-1}$ with relatively moderate volume expansion (<10%)[47][48][41].

There are critical performance problems, particularly with the initial Coulombic efficiency. ICE values are usually less than 80% in the absence of electrolyte

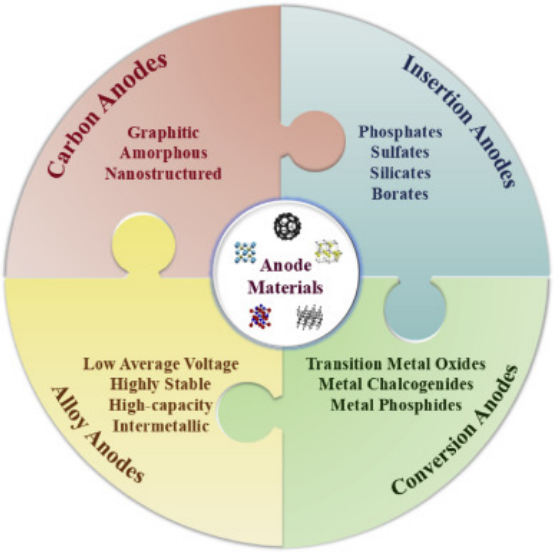

Figure 2.2: Types of anode materials
[46]

optimisation or pre-sodiation strategies. This is limited by permanent pore filling and irreversible Na^+ consumption as the solid electrolyte interphase (SEI) formation occurs. Recent work has demonstrated improvements in ICE to >90% by phosphorus doping strategies and optimised synthesis protocols[49].

MXenes ($Ti_3C_2T_x$ and counterparts) have a metallic conductivity and surface terminations, which are tunable, allowing the theoretical capacity in the range of 200-400 $mAhg^{-1}$. Practical application, however, is restricted due to the challenges such as interlayer restacking, surface termination complexity, and the constraints of synthesis in terms of etching operations and MAX phase availability[50].

2.2.4 Conversion Anodes

Conversion-type anodes permeate Na^+ through redox reactions to produce metal nanoparticles dispersed in $Na_2O/Na_2S/Na_3P$ matrices. While allowing for a higher theoretical capacity than intercalation materials, conversion anodes are lowered by inherent challenges, including high volume expansion (typically >100%), low electronic conductivity, and unstable SEI formation at the conversion potential[42].

Antimony conversion materials are an excellent example, as Sb_2O_3 microbelts exhibit quasi one-dimensional volume expansion mechanisms that improve cycling stability with capacities of 473.9 $mAhg^{-1}$ after 100 cycles. However, conversion

reactions remain only partially reversible, which causes first-cycle irreversible capacity loss as well as long-term stability problems[51].

2.2.5 Alloying Anodes

Alloying elements like Sn, Sb, Bi, and P form Na-rich phases (Na_3Sb, Na_3P) with theoretical capacities ranging from 100 -1000 $mAhg^{-1}$. The highest-capacity is with phosphorus, with a theoretical capacity of 2590 $mAhg^{-1}$, but practical application requires high amount of nanostructuring and carbon matrix incorporation[43].

The most significant challenge for alloying anodes is the colossal volume expansion that occurs upon cycling. Tin-based systems experience over 400% volume expansion throughout a full sodiation, and phosphorus anodes have 300-500% expansion. These expansions result in pulverisation of the particles, loss of electrical contact, and continuous SEI formation, which necessitate architectural designs, such as yolk-shell morphologies, carbon matrices, and nanosize active particles[43].

2.2.6 Challenges with existing anodes with sodium batteries

Low Initial Coulombic Efficiency in every anode class requires compensatory steps in the form of pre-sodiation additives (such as sodium acetate or sodium oxalate) or special proprietary electrolyte formulations. Every mitigation step incorporates materials, processing steps, and associated environmental footprints[52].

High-Temperature Processing requires control of energy use profiles. Certain hard carbon synthesis normally requires carbonisation at temperatures $\geq 800^oC$ for 2 to 4 hours, while conversion material preparation normally consists of calcination at 400-800^{o}C. Metal phosphide synthesis may entail additional high-energy ball milling or chemical vapour deposition processes[53].

Nanostructuration and Architectural Complexity improve electrochemical performance, but at twice the processing requirement. Advanced architectures, such as core-shell geometries, hierarchical porosity, heteroatom doping, and composite formation, require additional precursors, solvents, and multi-step processing routes[43].

Critical Element Dependencies vary by mechanism class. Conversion anodes will involve transition metals (Ni, Co, Fe, Mn), which have supply chain and toxicity issues. Alloying anodes depends on elements with limited availability, such as antimony and bismuth, which would preclude large-scale deployment.

Table 2.1: Summary of Key Challenges by Anode Type

Anode Type	Key Challenges	Source
Alloy-based	• Severe volume expansion (>200%) causes electrode pulverisation and low ICE. • Slow alloying kinetics limit rate performance, requiring nanosizing/carbon composites to buffer strain.	[23]
Conversion-based	• Large volume swings (>100%) and unstable SEI drive capacity fade and low ICE. • Poor conductivity and multi-phase conversion pathways cause voltage hysteresis and polarisation.	[54]
Intercalation-based	• Low theoretical capacities ($\leq$ 350 $mAhg^{-1}$) and limited conductivity hinder rate capability. • Side reactions (H_2 evolution, dissolution), finite Na^+ sites, and heavy polyanions reduce energy density.	[55]

2.3 Life-cycle assessment results and implications for the LCA community

The evolution of sodium-ion batteries must be accompanied by thorough life-cycle assessments (LCAs) to ensure that the transition away from lithium does not simply shift impacts to other parts of the supply chain. Preliminary LCAs of SIBs already single out the negative electrode as a major hotspot, yet most studies to date consider a narrow set of anode materials-typically hard carbons-and make simplifying assumptions for the other cell components. This thesis closes that gap by providing a broader, data-heavy list of nine anode materials [23].

2.3.1 Available LCA results for sodium-ion battery anodes

The statement of the first cradle-to-gate LCA of a sodium-ion cell by Peters et al. (2016) [23] modelled a battery with a layered oxide cathode and a hard-carbon anode derived from sugar. Their open inventory revealed that anode production

was one of the highest contributors to several impact categories, accounting for roughly 24% of the global warming potential of the entire cell. The sugar precursor contributed around 17% of total GWP owing to the energy and land intensity of sugar production. The inert pyrolysis atmosphere (achieved using nitrogen gas) and use of aluminium current collectors also represented notable burdens. A sensitivity analysis showed that substitution of the sugar with organic waste or petroleum coke could greatly reduce impacts; use of organic waste lowered GWP by approx. 16% and marine eutrophication by up to 62%. The authors summarised that the synthesis of low impact hard carbon and developing energy efficiency in cell manufacturing are high priorities.

More recently, Wickerts et al. (2024)[24] performed a prospective LCA on two sodium-ion cells that had been designed for large-scale manufacture. Both cells featured a Prussian-white cathode and hard-carbon anode, but differed in that the first contained a phenolic-resin hard carbon and the second a lignin-based hard carbon. They concluded that no single hotspot is dominating; instead, the impacts are spread throughout anode and cathode production, gigafactory energy usage, electrolyte production and current collectors, whereas binders and separators contribute negligibly. The lignin-based anode was found to have lower global warming and fossil resource depletion than the phenolic-resin anode when mass allocation was applied. The investigation did, however, emphasise that allocation choices (mass-based or "main-product-bears-all-burden") significantly influence the determined hard carbon contribution. If the lignin-based anode carries all pyrolysis and pulp production burdens, its impact is near that of the phenolic resin anode. The authors therefore proposed the supply of fossil-free electricity for cell manufacturing and further investigation of low-impact electrolytes[24].

Additional evidence comes from a comparative LCA of bio-derived hard carbon anodes published by Liu et al. (2021). Two routes were compared: hydrothermal carbonisation and pyrolysis versus direct pyrolysis of biomass. Both routes lowered environmental impacts considerably compared to conventional hard carbon: the hydrothermal route lowered global warming potential by around 30%, while the direct-pyrolysis route lowered it by approx. 21%. Toxicity, photochemical oxidant formation, acidification and eutrophication also improved. These results illustrate the potential to mitigate impacts without compromising good electrochemical performance through the use of bio-derived precursors and enhanced processing[56]. Various current LCAs on the sodium battery are compiled in the below Table 2.2[57].

Table 2.2: Global Warming Impact of Different Battery Materials (CO_2 eq)

Reference	**Active Material**	**Functional Unit**	**Global Warming Potential**
Peters et al., 2016 [23]	Cathode: $Na_{1.1}Ni_{0.3}Mn_{0.5}Mg_{0.05}Ti_{0.05}O_2$ Anode: Hard carbon	kW storage capacity	140.33 kg CO_2eq/kW
Peters et al., 2019 [58]	Anode 1: Hard carbon from waste tires Anode 2: Hard carbon from apple pomace Anode 3: Hard carbon from phenolic resins	kg hard carbon kg SIB cell	6.27 kg CO_2eq 10.41 kg CO_2eq 2.69 kg CO_2eq (hard carbon from apple pomace) 9.42 kg CO_2eq (SIB cell) 14.85 kg CO_2eq (hard carbon) 12.78 kg CO_2eq (SIB cell)
Peters et al., 2021 [54]	Cathode 1: $Na_{1.1}Ni_{0.3}Mn_{0.5}Mg_{0.05}Ti_{0.05}O_2$ (NaNMMT) Cathode 2: $Na_{2/3}(Mn_{0.95}Mg_{0.05})O_2$ (NaMMO) Cathode 3: $Na_{1.05}(Ni_{0.33}Mn_{0.33}Co_{0.33})_{0.95}O_2$ (NaNMC) Cathode 4: $Na_2[Fe(CN)_6]$ (NaPBA) Cathode 5: $Na_4[MnV(PO_4)_3]$ (NaMVP) Anode: Hard carbon	kWh of battery cell capacity	50.6 kg CO_2eq 52.3 kg CO_2eq 86.7 kg CO_2eq 87.0 kg CO_2eq 89.7 kg CO_2eq
Malara et al., 2021 [59]	Anode 1: Electro-spun Fe_2O_3:Si-based fibers Anode 2: Electro-spun Fe_2O_3-based fibers	storage capacity delivered by the anode	-

(continued on next page)

(continued from previous page)

Reference	Active Material	Functional Unit	Global Warming Potential
Liu et al., 2021 [56]	Anode 1: HTC + pyrolysis Anode 2: Direct pyrolysis	kg hard carbon	4.07 kg CO_2eq 4.61 kg CO_2eq
Mozaffarpour et al., 2022 [60]	Cathode 1: $Na_3MnCO_3PO_4$ (ball milling) Cathode 2: $Na_3MnCO_3PO_4$ (hydrothermal) Cathode 3: $Na_3MnCO_3PO_4$ (stirring-assisted hydrothermal)	kg hard cathode	15.3 kg CO_2eq 14.2 kg CO_2eq 20.0 kg CO_2eq
Carvalho et al., 2022 [61]	Na_Lab and Na_Ind - Cathode: $Na_{0.44}MnO_2$/Anode: Mxene-$Ti_1Al_1TiC_{1.85}$	kWh coin cell capacity	5.56×10^4 kg CO_2eq (Na_Lab) 6.98 kg CO_2eq/kg coin Na_Lab 5.15×10^3 kg CO_2eq (Na_Ind) 2.21 kg CO_2eq/kg coin Na_Ind

2.3.2 Current studies' limitations and data gaps remaining

Informative though they are, LCAs currently available lack from the following shared limitations:

- Narrow scope of anode materials. The majority currently evaluate only hard-carbon anodes, with alloying and conversion materials remaining unstudied. For instance, neither the 2016 nor the 2024 LCAs include tin, antimony, phosphorus, iron oxide, or MXene anodes, which prevail in current laboratory studies.

- Generic or simplified inventories. The process data from the lab scale and generic proxies for some chemicals were used in the 2016 study, while the future 2024 LCA relied heavily on projected gigafactory data and general assumptions about the upstream processes. Functional units or anode production system boundaries are not consistent across studies.

- Energy sourcing and allocation sensitivity. Wickerts et al. [24] showed that

allocation rules and power mixes can shift the relative importance of the anode. In the absence of standard inventories, it is challenging to scale results to new cases or compare different alternative anode materials.

- Lack of manufacturer data. With the exception of the Prussian-white cathode data in this 2024 study, no LCA has utilised direct data from industrial sodium-ion anode manufacturing. This excludes providing assurance for comparison reliability as well as hotspot identification in the real world.

2.3.3 Relevance of this study

This thesis directly addresses these gaps. Through combining process data from a broad range of experimental investigations and constructing a normalised life-cycle inventory (LCI) for nine anode materials, it will enable more comprehensive LCAs of sodium-ion batteries. In contrast to earlier work focusing on hard carbon only, the proposed LCI will encompass intercalation, conversion and alloying anodes-from hard and soft carbons to red phosphorus, tin and antimony composites. All inputs (precursors, solvents, energy needed) will be normalised to a gram-based functional unit and converted to ecoinvent proxies where necessary, with open data accessible for LCA practitioners to convert to alternative system boundaries and allocation methods. In the ambit of existing LCAs, this meta-analysis will therefore:

- Expanding the environmental knowledge base beyond hard carbon, allowing future LCAs to compare anodes on a level playing ground and outline truly sustainable choices.

- Improve data quality and consistency via documentation of assumptions, yields and uncertainties, to enable sensitivity analysis and harmonisation of studies.

- Facilitate modelling in the future of industrial-scale anode production, by enabling input–output datasets that can be integrated with renewable electricity scenarios and models of manufacturing energy.

In brief, present LCAs emphasise that anode production can be a profitable environmental hotspot but do little to inform how comparative alternative anode chemistries and synthesis routes correlate with each other. By compiling an exhaustive and harmonised database of sodium-ion anode inventories, this thesis will provide the LCA community with the means needed to make more accurate judgements of sustainability and guide the development of future batteries.

Chapter 3

Methodology

3.1 Compilation of Anode Active Material Inventory Dataset

The inventory compilation of the anode active material inventory is an important step in this study, as it builds the foundation for the subsequent life cycle inventory (LCI) construction and environmental impact assessment. This section ensures that the selected anode materials are not only high-performing from an electrochemical standpoint.

3.1.1 Selection of anode active materials

The anode materials chosen for this research represent some of the leading classes of sodium-ion battery (SIB) negative electrodes, selected through a literature review and the comparison across the articles according to the following criteria[46][14][62][63]:

1. High Theoretical capacity: Ensures competitive energy storage potential and informs the upper bound of device performance;
2. Good reversible capacity: Demonstrates practical and stable Na^+ storage over repeated cycles, confirming material utility in real-world scenarios;
3. Cycling stability: Reflects long-term durability, frequently validated over 500 or more cycles, and is essential for commercialisation.

From the insights gained from the work of Peters et al. 2016[23], Peters et al, 2021[54], Sharmin et al, 2024 [46] and Wand et al, 2024[14] the anodes selected for this study exemplify the most relevant advances for practical, high-performance sodium-ion energy storage.

Hard Carbon (Biomass and Petroleum Coke-Derived)

Hard carbon (HC) is the reference anode for sodium-ion batteries (SIBs) due to its low sodiation potential (<0.2 V vs Na/Na^+), viable reversible capacity (250–350 $mAhg^{-1}$), and documented lifespan of 1000–2000 cycles under optimised conditions. Biomass-derived hard carbons produced from renewable feedstocks, such as lignin or nutshells, offer both lower environmental impacts and high electrochemical performance. The hierarchical porosity enables both adsorption of Na^+ and pore-filling, resulting in high capacities and high rate performance. Petroleum coke-based HC provides robust, industrially significant baselines and robust, reproducible synthesis conditions, as evidenced by life cycle analysis by Peters et al. The scalability of both approaches either industrial waste or sustainable places hard carbon ideally for the economically feasible mass production of SIB anodes[64][57][54][23].

Sb_2O_3

Antimony oxide (Sb_2O_3) operates in a conversion mode, reducing with sodium to produce Na_3Sb, with a theoretical capacity of 660 $mAhg^{-1}$. Usual drawbacks are large volume change and mechanical degradation; despite this, recent advances in nanoengineering and carbon compositing have provided reversible capacities of approximately. 450 $mAhg^{-1}$ with cycling stability of over 200 cycles with improved retention. The ongoing progression of composite and nanostructured Sb_2O_3 arrangements makes this material a tunable, high-capacity anode, ready for further upscaling[24][55].

Fe_2O_3 and Fe_3O_4

Iron oxides, e.g., Fe_2O_3 (hematite, 1007 $mAhg^{-1}$) and Fe_3O_4 (magnetite, approx. 926 $mAhg^{-1}$), possess natural abundance, low toxicity, and costliness, and are, therefore, extremely desirable for green and sustainable storage. Key issues, low electronic conductivity and unstable SEI are increasingly overcome by materials strategies such as hollow/multishelled morphologies and graphene integration, which now routinely register reversible capacities of 400–500 $mAhg^{-1}$ along with cycling stabilities of over 500 cycles. Their eco-friendly nature and versatility make it easier to transition from laboratory prototype to large-scale SIB production.[59][65]

Bi_2Sb_6

Bismuth–antimony alloys such as Bi_2Sb_6 leverage the mechanical strength of Bi and the superior sodium-storage property of Sb to achieve synergetic improvement in cycle life and capacity retention relative to pure Sb. The alloys demonstrate

reversible capacity stability (400 $mAhg^{-1}$) and approximately 85% capacity retention at 300 cycles, which suggests a potential for commercial cells where energy density, along with durability, is of prime concern. Alloy design versatility favours subsequent optimisation and scale-up opportunities.[66]

Multi-Channel Red Phosphorus Nanotubes (MCRPNTs)

Red phosphorus features a record-high theoretical capacity (2596 $mAhg^{-1}$) but is hindered by extreme critical issues like extremely low electrical conductivity and catastrophic (approx. 300%) volume expansion. Multi-channel nanotube structures alleviate the mechanical accommodation and electrical connectivity problems needed to deliver useful capacities (1000–1500 $mAhg^{-1}$) with decent stability (>200 cycles). These results shows that despite synthetic complexity, next-generation phosphorus architectures hold promise for disruptive, high-capacity SIB anodes.[67]

MXenes ($Ti_3C_2T_x$ and related)

MXenes belong to a family of 2D transition metal carbides/nitrides with high electronic conductivity and tunable surface properties. Specifically, Ti-based MXenes (e.g., $Ti_3C_2T_x$) support rapid sodium-ion intercalation and pseudocapacitive storage, with capacities of 200–400 $mAhg^{-1}$ and extremely long lifetimes (>1000 cycles) reported. The solution-processability, high rate performance, and chemical modifiability of MXenes make them especially attractive electrodes for fast-charging, scalable SIBs.[68]

Sn with Carbon Nanofibers (Sn@CNF)

Tin (Sn) anodes possess high theoretical capacity (847 $mAhg^{-1}$) but are inherently plagued by extensive volume changes during cycling. Submergence of Sn nanoparticles in flexible carbon nanofibers mitigates these mechanical stresses, suppresses pulverisation, and maintains electronic connectivity. Composites such as these spontaneously deliver stable, reversible capacities of 400–500 $mAhg^{-1}$ for over 500 cycles and therefore introduce Sn@CNF hybrids as a scalable and feasible alloy–carbon anode proof-of-concept for SIBs.[69][70]

Sn_4P_3

The Sn–P alloy Sn_4P_3 combines the high theoretical capacity of phosphorus (2596 $mAhg^{-1}$) with tin's improved conductivity, achieving a balanced theoretical capacity of 1132 $mAhg^{-1}$. Reversible capacities of 700–800 $mAhg^{-1}$ were realised over 300+ cycles, and the relatively low sodiation potential enhances SIB cell voltages.

Scalability and performance of this alloy structure position Sn_4P_3 as a top contender for future SIB anodes[71].
To make it easier to compare the selected anodes, a comparison table has been put together, with a summary as shown in Table 3.1. This table shows their theoretical capacities, reported reversible capacities, cycle stability, and key references. It is interesting to note that while the various materials have their own strengths and weaknesses, such as some having high energy density and others excelling in structural stability, each anode included has the potential to scale up to the next stage from the lab scale level. There are many other anode active material research available, given the scope, these anode materials were analysed for the database development.

Table 3.1: Performance of Sodium-Ion Battery Anodes

Anode Material	**Type**	**Voltage vs Na/Na^+ (V)**	**Theoretical Capacity (mAh g^{-1})**	**Reversible Capacity (mAh g^{-1})**	**Cycling Stability**	**Source**
Hard Carbon (biomass)	Intercalation	<0.2	300–350	250–350	>2000 cycles (optimized)	[46]
Hard Carbon (petroleum coke)	Intercalation	<0.2	300–350	250–300	>1000 cycles	[46]
Sb@C-composite	Conversion	0.01–2.5	∼660	200∼450	>200 cycles (with carbon composite)	[72]
Fe_2O_3	Conversion	0.01–3.0	∼1007	400–500	>500 cycles (with nanostructuring)	[59]
Fe_3O_4	Conversion	0.01–3.0	∼926	200–500	>1000 cycles (graphene/hollow structures)	[73]
Bi_2Sb_6	Alloy	0.01–2.5	150-300	∼400	∼2000 cycles, ∼85% retention	[66]
Multi-Channel Red P Nanotubes	Alloy (P-based)	0.01–2.0	2596	1000–1800	>100 cycles	[74]
MXenes ($Ti_3C_2T_x$)	Intercalation	0.01–3.0	200–400	200–400	>1000 cycles	[61]
Sn@CNF	Alloy	0.01–2.5	847	200-400	>1000 cycles	[75]
Sn_4P_3	Alloy	0.01–2.5	1132	700–800	>300 cycles	[76]

3.1.2 Electrochemical Parameters for Anodes

To enable systematic comparison between the different anode materials and to ensure consistency in LCI preparation, an index list of electrochemical parameters was created. SIB anode research is reported in different forms across the literature with a variety of testing conditions, cut-off voltages, current densities, and reporting formats. This diversity both complicates performance benchmarking and sustainability analysis in the absence of harmonisation. The index list thus provides a harmonised set of electrochemical data as a bridge between meta-analysis of experimental studies and LCI database creation.

Parameters addressed by the index list

1. Theoretical capacity ($mAhg^{-1}$): Theoretically absolute maximum of electrical charge that active materials of a battery can store and deliver under ideal, perfect circumstances, calculated according to Faraday's law and under the assumption that all active particles participate fully in the electrochemical reaction. Calculated from the mechanism of the chemical reaction, showing the theoretical maximum Na^+ storage per unit mass.

2. Reversible (practical) capacity ($mAhg^{-1}$): The energy that is available to be stored in repeated charge-discharge cycles, and which is the repeatable, stable energy available from an electrode after initial formation cycles. Measured experimentally by standard cycling conditions.

3. Initial Coulombic Efficiency (ICE, %): First-discharge charge extracted over first-charge charge delivered, in terms of ampere-hours (Ah). Measure of first-discharge capacity compared to first charge capacity to reveal initial loss of Na^+ and SEI formation.

4. Average potential vs. Na/Na^+ (V): Average working voltage, which has a significant effect on the overall energy density of a full cell.

5. Cycling stability (cycle number and retention): The ability of a battery to maintain performance, specifically capacity and life, following many charge/discharge cycles. Tendency to be expressed as % retention following the number of cycles.

3.2 Anode Inventory Compilation

Building a detailed inventory database for sodium-ion battery (SIB) anode materials is essential due to the diversity of novel anode chemistries and the lack of existing life-cycle data. Unlike lithium-ion batteries (LIBs), SIBs cannot use

graphite effectively, so researchers are exploring a wide range of alternative anodes including intercalation types hard carbon and novel 2D materials like MXenes, alloying metals (Sn, Sb, Bi), conversion-type oxides/sulfides/phosphides (Fe_2O_3, Fe_3O_4, Sn_4P_3, etc.). Studies to date have focused on electrochemical performance, often neglecting environmental aspects; consequently, LCA studies on the production of these SIB anode materials are limited. Establishing an inventory of lab-scale synthesis processes allows for evaluating and comparing the environmental impacts of these materials and supporting future eco-design of SIB cells.

To compile the anode inventory dataset, synthesis data have been gathered for selected anode materials from experimental literature (lab-scale studies). Each material's preparation route was carefully reconstructed from reported procedures, including all input materials (precursors, solvents, reagents), process conditions (atmosphere, temperature, duration), equipment and energy-intensive steps, and output yields or losses. When specific details did not explicitly report certain information (e.g. exact yields, energy usage, or minor inputs), reasonable estimates were made, such as assuming complete conversion of limiting reagents if yields were not given, or calculating furnace energy consumption based on temperature profiles and batch size.

Although there are various synthesis methods and approaches for a particular chemistry, in this section, an explanation of the procedure is given for the methods that the scientific article proposed.

Each inventory line item was then mapped to an appropriate process in the ecoinvent v3.11 LCI database for consistency in LCA modelling, if an exact match was unavailable, an upstream production proxy was created using available ecoinvent flows. The compiled data were checked in LCA software (openLCA) to ensure all flows are valid. In the following, the anode materials are grouped by their primary synthesis method: pyrolysis, mechanochemical ball milling, solvothermal/hydrothermal synthesis, electrospinning, chemical dealloying, and selective etching – and the details of each synthesis procedure are described. Also, highlighting any process-specific emissions or hazards (e.g. HF usage, phosphorus vapours, solvent losses) that were accounted for in the inventory.

3.2.1 Pyrolysis-Derived Anode Materials

Carbon based anodes

Pyrolysis (thermal decomposition under an inert or controlled atmosphere) is the predominant method to synthesise carbon based SIB anodes and certain composite materials. Hard carbon, the standard SIB anode, is typically synthesised via pyrolysis of organic precursors (biomass, polymers, resins, etc.) under high-temperature

conditions (generally 800–1200^{o}C) under an argon or nitrogen environment. This operation volatilises the volatile constituents and yields a carbon-rich char[77]. The significant inputs are the precursor (which is typically dried out to remove moisture) and a flowing inert gas stream (to prevent oxidation). The process is energy-intensive due to the high furnace temperatures and long dwell times (hours) that we account for in the inventory, which result in significant electricity or fuel demand. The product is typically a hard, powdered carbon, with yields dependent on the precursor. Carbon yield in the case of biomass precursors can be of the order of 20–40% of weight; the yield could be lower or higher percentages depending on their construction and ash content. For instance, in the manufacturing of 1 kg hard carbon from phenolic resin, it has been found to emit a much larger GHG footprint (14.85 kg CO_2-eq) than that from an amount of biomass-based feedstock like apple pomace (2.69 kg CO_2-eq), suggesting differences in the yield of carbon and energy consumption during the process[78][61][79].

In some biomass-based anodes, a two-step process is used: e.g., hydrothermal carbonisation of biomass at 200^{o}C in an autoclave to yield a hydrochar, followed by high-temperature pyrolysis to yield a hard carbon. These integrated routes can enhance carbon yield and mitigate environmental impact over single-step direct pyrolysis. Liu et al. (2021)[56] demonstrated that HTC + pyrolysis of biomass resulted in lower GHG emissions, human toxicity, and photochemical ozone formation compared to direct pyrolysis of the same biomass[79].

3.2.2 Solvothermal derived anode materials

Red Phosphrous

In the synthesis of phosphorus-based anodes, anodes are prepared through solution-mediated reactions under controlled conditions. A well-known example is the preparation of multi-channel red phosphorus nanotubes (MCRPNTs) in recent work. Here, first a 0.04 M dispersion of phosphorus triiodide (PI_3) is dissolved in 5 mL iodobenzene. In the same time 0.02 M cetyltrimethylammonium bromide (CTAB) is dissolved in ethylene glycol. Iodobenxine is then added dropwise into mixture of CTAB with constant agitation for approximately 15 minutes, which causes the medium color to change from reddish-brown liquid to reddish-orange precipitate. The so-obtained dispersion is filled in an autoclave and heat-treated at 180^{o}C for varying times (typically 90 or 120 min), producing mid-term products subsequently identified as MRPN-3 based on the treatment time. When cooled to room temperature, through centrifuge precipitate is separated, washed several times with acetone and ethanol to eliminate residual by-products, and re-dispersed in absolute ethanol for further purification. The resultant end powders are obtained

after vacuum drying at 200 °C for 5 hours and deliver multi-channel red phosphorus nanotube anodes with high specific capacities as well as better cycling stability[74].

Sn_4P_3

The inputs for the synthesis are $SnCl_2 \cdot 2H_2O$, commercial red phosphorus powder, rGO suspension, and ethanolamine as a solvent. The energy demand is dominated by autoclave heating at 180^oC for 15 h. The resultant suspension is transferred into a Teflon-lined stainless steel autoclave, sealed airtight and then maintained at 180^oC for 15 h under autogenous pressure conditions. Outputs are the Sn_4P_3–rGO composite powder (with near-quantitative precursor to product conversion) and liquid waste streams of ethanol and water used in washing. These losses of solvents incurred during washing and ultrasonication are estimated as volatile organic emissions[76].

3.2.3 Ball milling based anode materials

Mechanochemical synthesis via ball milling is another route used to create SIB anode materials, especially alloy or composite anodes. High-energy ball milling involves grinding powders together in a milling vessel, using hardened balls (e.g. tungsten carbide or stainless steel) to impact and cold-weld/fracture the materials repeatedly. This can induce chemical reactions or intimate mixing at room temperature without the need for solvent or furnace steps.

Sb/C composites

The synthesis of Sb/C composites include antimony and CaC_2 powders which are the main inputs are then combined in controlled mass ratios, with 1:1 with argon for the protective milling environment, hydrochloric acid, water, and electricity for prolonged high-speed milling. It is first subjected to a preliminary milling step to reduce particle size and enhance reactivity with ball-to-powder weight ratio of 20:1. The Sb/C composite is then synthesised in an aqueous waste streams containing Ca^{2+} and chloride ions, and the release of acetylene gas (C_2H_2) during the hydrolysis of unreacted CaC_2 in acidic medium.[72]

Sn/C nano composite

The anode is synthesised in stages. First stage, the precursor powders were mechanically processed to obtain the active negative material: tin metal powder for the Sn anode, and a mixture of tin powder with carbon nanofibers for the Sn–NC composites. The powders are placed in tungsten carbide jars and subjected to high-energy ball milling, with an additional milling to ensure thorough mixing and

homogenisation. In the second stage, the resulting active material was blended with a polymeric binder dissolved in an appropriate solvent and supplemented with carbon black (C65) as a conductive additive. Sn–NC_CMC, employing carboxymethylcellulose (CMC) in water, is prepared[61].

3.2.4 Electrospun nanofiber anode materials

Electrospinning is used to create nanofiber mats that serve as anode materials (often metal oxide or carbon nanofiber composites). The general procedure for electrospun anodes involves[80][81]:

1. Preparing a viscous polymer solution containing the precursor of the active material

2. Electrospinning the solution into fibre form

3. Post-treatment of the fibre mat (calcination or carbonisation) to obtain the final active material embedded in or constituting the fibres.

Fe_2O_3

Synthesis of Fe_2O_3 anode active material, the principal inputs include polyacrylonitrile (PAN), N,N-dimethylformamide(DMF), $FeAc_2$, tetraethyl orthosilicate (TEOS) (the ratio of composition is as shown in the)with argon gas is magnetically stirred and electrospun using high voltage spinner during which most of the solvent rapidly evaporates to yield non-woven fibrous membranes, dilute hydrochloric acid (for subsequent leaching), deionized water, and energy consumption associated with high-voltage spinning and furnace operation, while outputs consist of the targeted Fe_2O_3-based nanofiber product, evaporated DMF and gaseous emissions, as well as acid effluents containing dissolved calcium species.[65]

Fe_3O_4

For preparing transition-metal-oxide composite, the general process is to dissolve polyvinylpyrrolidone (PVP) and metal chloride precursor ($FeCl_3$, $ZnCl_2$, or $MnCl_2$) in N,N-dimethylformamide (DMF), followed by stirring at 60^oC for 2 h. Then, polyacrylonitrile (PAN) is added, and the solution is stirred intensively for another hours to get a homogeneous precursor solution for electrospinning. The solution was subsequently electrospun with fibers collected on a rotating aluminum foil collector. The as-spun membranes were peeled off immediately and carbonized in 600^oC for 2 h in nitrogen (heating rate of $1^oC\ min^{-1}$), leading to flexible nanofiber termed as uf-Fe_3O_4@N-CNFs respectively[65].

3.2.5 Chemical Dealloying Derived Anodes

Chemical dealloying is a method to produce nanoporous metal or intermetallic anodes by selectively dissolving one element from an alloy.

Bi_2Sb_6

The nanoporous Bi_2Sb_6 alloy is generally produced by a melt-spinning and dealloying path. A ternary precursor with the nominal composition is first created by melting high-purity Mg, Bi, and Sb blocks (99.9 wt%) in concert in a graphite crucible at 740^oC for 30 min using an electric resistance furnace in a protective flux. The molten alloy is then cast into a mold to create an ingot, which is after that shaped by a single-roller melt spinner at 1000 rpm in an argon environment to obtain rapid solidification into thin foils. The foils are after that treated with chemical dealloying in 2 wt% tartaric acid at room temperature and the reaction continued until gas evolution ceases, showing complete removal of Mg. Dealloyed samples were thoroughly rinsed with deionised water and ethanol to eliminate the remaining salts and acids and vacuum dried at 60^oC for 5 h to yield the resultant nanoporous Bi_2Sb_6 alloy[66].

3.2.6 Selective etching method for Mxenes

MXenes represent a family of two-dimensional materials comprising transition metal carbides, nitrides, or carbonitrides with better electrical conductivity, surface chemistry modifiability, and prospective electrochemical properties that render them as favourable candidates to be employed in sodium-ion batteries. MXenes are generally synthesised through selective etching of "A" layers, typically aluminium, silicon, or gallium, in the precursors to layered MAX phases. This process produces atomically thin nanosheets with a typical composition of Mn+1XnTx, where "M" is a transition metal, "X" is carbon or nitrogen, and "Tx" is surface functional groups of –O, –OH, and –F. The etching removes the weaker metal-A bonds of the MAX phases but leaves the stronger metal–carbon or metal–nitrogen bonds that form the MXene structure[50].

There are several etching methods for MXene synthesis, broadly classified into "top-down" processes in which the "A" layers are removed chemically or electrochemically and "bottom-up" processes, which encompass direct synthesis methodologies such as chemical vapour deposition. The most common top-down etching method is the use of hydrofluoric acid (HF) or fluoride-based counterpart mixtures to dissolve the "A" layers to yield MXenes with surface terminations that dictate their electrochemical characteristics. In response to issues of unsafe HF use, various less reactive and fluorine-based etchants such as alkali solutions, halogens,

molten salts, and electrochemical etching have been engineered. Every synthesis route influences the structure, surface chemistry, interlayer spacing, and stability of the obtained MXene. Such a synthesis route flexibility allows the capability of designing MXenes for their best application in sodium-ion batteries and other applications.[50]

3.3 Validation of Inventory data through simplified LCA

3.3.1 Goal and Scope definition

The primary goal of this study is to validate selected sodium-ion battery (SIB) anode active material aggregated life cycle inventories (LCIs) through a condensed life cycle assessment (LCA). Although comprehensive-scale anode and full cell comparative life cycle assessment falls outside the present scope, preliminary validation is essential to determine the database's validity, completeness, and internal consistency developed in subsection 3.1.1. This step ensures that the compiled lists are likely to be incorporated into future SIB system evaluations firmly and contrasted on a variety of chemistries.

Since the present study is underway using laboratory-scale synthesis data, the boundary is considered to be cradle-to-lab-gate. This boundary starts with raw material excavation and processing (e.g., biomass feedstocks, metal precursors, solvents) and includes all lab-scale processing operations like grinding, pyrolysis, solvothermal processing, electrospinning, and after-synthesis washing or drying. The boundary ends at the point where anode active material is produced and ready to be utilised in downstream electrode preparation. The subsequent steps- cell assembly, battery use, and end-of-life are out of scope of the existing analysis, as per the future LCA's strategy for novel battery technologies.

Data from the previous study from Peters et al. 2021[54] is also used for a comparison, as a benchmark of this study. The inventory data from the previous study is used with an updated LCA database, to observe how the environmental impact would change with the same inventory but at a more modern production scenario

Geographical scope of study

To evaluate the environmental impacts of sodium-ion battery production, three different geographical contexts were selected: India, Europe, and a model without a location. The selection was based on the following considerations:

- India was chosen as a case of an emerging economy with a rapidly growing energy demand and a high reliance on coal in its electricity mix[82]. Including India highlights the effects of battery production in a carbon-intensive context.
- Europe was included with two scenarios: one using the regular energy mix (representing the current grid average) and one with a renewable energy mix (representing a low-carbon scenario). This allows for comparison between present conditions and potential future improvements in energy sourcing.
- A case of 'no location' is considered, allowing the model to run freely and assess the impact with no constraints on the production of the anode active material.

3.3.2 Functional Unit

The definition of a functional unit is a critical step in life cycle assessment (LCA), as it establishes the reference against which all material and energy flows are quantified. In this study, the functional unit was defined as 1 kg of sodium-ion battery (SIB) anode active material produced at the laboratory scale, i.e., at the cradle-to-lab-gate boundary.

3.3.3 Impact Assessment and LCI Database

Impact Assessment and LCI Database

The LCIA methodology, which has been selected for this research, is the ILCD 2011 Midpoint+ method. The ILCD was conceived by the European Commission to provide harmonised guidance towards conducting LCA studies[83]. The ILCD 2011 Midpoint+ approach employs 16 categories at the midpoint level, i.e., it evaluates environmental interventions at a place somewhere between the cause–effect sequence of elementary flows (e.g., CO_2 emissions) and final damage categories (e.g., human health, ecosystem quality)[**comparision**][84]. In practice, midpoint categories correspond to specific environmental problems such as climate change, acidification, or eutrophication, rather than endpoint aggregations.

Of the ReCiPe 2016 midpoint indicators, two were selected for this validation step: abiotic depletion potential(ADP)/Resource depletion and global warming potential (GWP). These indicators were also selected because they are of high relevance to the environmental performance of battery technologies, and mostly based on these parameters, scaling up of the technology is considered from the current context of a net-zero emissions perspective. They also directly address the most pertinent sustainability challenges of anode synthesis: the energy-intensive character of dense lab-scale processes and raw material depletion through key

critical raw materials.

Global Warming Potential (GWP) specifies the ability of greenhouse gas (GHG) emissions (CO_2, CH_4, N_2O, etc.) to influence climate change, in kg CO_2-equivalents.

Abiotic Depletion Potential (ADP) is an expression of utilisation of non-renewable abiotic materials, e.g., fossil fuels, minerals, metals, normalised against an availability reserve, and expressed in units of kg Cu-equivalents[85].

The life cycle inventory (LCI) database employed throughout this work is Ecoinvent v3.11, which at the time of conducting this work (published November 2024) was the most recent and largest LCI database available[86]. Ecoinvent includes comprehensive process-level inventories of chemicals, energy carriers, and industrial processes, and is therefore particularly well adapted to laboratory-scale data mapping. A key update in this release is the inclusion of the 2021 dataset-based electricity generation mix, which better reflects the carbon intensity of power consumption than earlier releases[87].

All LCA calculations for model and validation were conducted using the OpenLCA software, version 2.5[88], which is ReCiPe 2016, midpoint (H) and Ecoinvent dataset supportive.

The approach taken in this simplified validation's methodology is presented in Table 3.2.

Table 3.2: Summary of LCA Methodological Setup

System Boundary	Cradle-to-Lab-Gate (raw materials → lab-scale anode synthesis)
Functional Unit	1 kg of anode active material produced
Impact Assessment Method	ReCiPe 2016, midpoint (H)
Selected Impact Categories	1) Global Warming Potential (GWP) 2) Abiotic Depletion Potential (ADP)
LCI Database	Ecoinvent v3.11 (released Nov 2024)
LCA Software	OpenLCA version 2.5

3.3.4 Data Collection

The life cycle inventory (LCI) data for the selected anode active materials mainly follows the synthesis descriptions explained in the previous section 3.2. For hard carbon, the inventory was developed using the study of Peters et al. (2021) [54] as a key reference to assess and understand the environmental implications of large-scale production. For the other anode materials, the inventory data were compiled directly from the synthesis methodologies reported in research articles.

Where specific precursors or processing steps were not available in the ecoinvent v3.11 database[87], the missing items were generalised to the closest available proxies in order to enable this preliminary assessment. A full list of the inventory data, including mapping to ecoinvent processes, is provided in the Appendix.

For energy inputs, electricity from a medium voltage supply was selected as the reference source, while for thermal requirements, a small-scale central heat source was adopted. To ensure geographical consistency, the entire inventory was modelled under the European regional context, aligning with the electricity and heat mixes available in the latest ecoinvent datasets.

Chapter 4

Results and Discussions

4.1 LCI and LCA analysis

The results of the standardised life cycle assessment of the selected anode materials are expressed on a global warming potential (GWP) and abiotic resource depletion potential (ADP) basis. Figure 4.1 shows the relative performance of anodes for different geographical and electricity-mix scenarios: India, Europe (mixed grid), Europe (renewable-intensive grid), and a location that is not disclosed.

The rationale behind this decision is two-fold. India is added for the first time as a proxy for the new manufacturing hubs, where the generation of electricity is still largely fossil fuel-based, with the largest share accounted for by coal (45%)[82]. The result clearly indicates that the Indian grid mix accounts for considerably higher GWP values than the other components. On the other hand, Europe was chosen as the reference due to its ongoing pursuit of self-sufficiency in battery manufacture and its progressive use of renewable integration. The outcome shows that on the basis of a renewable-dominant European grid mix, the GWP values of all the anodes decrease substantially from the mixed European grid, which highlights the contribution of decarbonising the electricity supply. The unannounced location case was conducted as a sensitivity case with no geo-restrictions. Interestingly, the result emphasised rather moderate differences from the European renewable case, justifying that clean electricity mixtures are the most significant driver towards lower GWP.

Even the anode material composition proved to be a significant driver for environmental performance as shown in the Figure 4.1 for a case of Europe with renewable energy. In particular, emissions of some solvents were revealed to dominate the emission profile: the highest contribution of GWP in Fe_2O_3 and

Fe_3O_4 synthesis routes was caused by dimethoxyethane (DME). Similarly, energy-intensive and high-temperature synthesis routes, like that of hard carbon derived from biomass and multi-channel red phosphorus nanotubes (MRPNs), increased the GWP significantly due to electricity-consuming furnace operations.

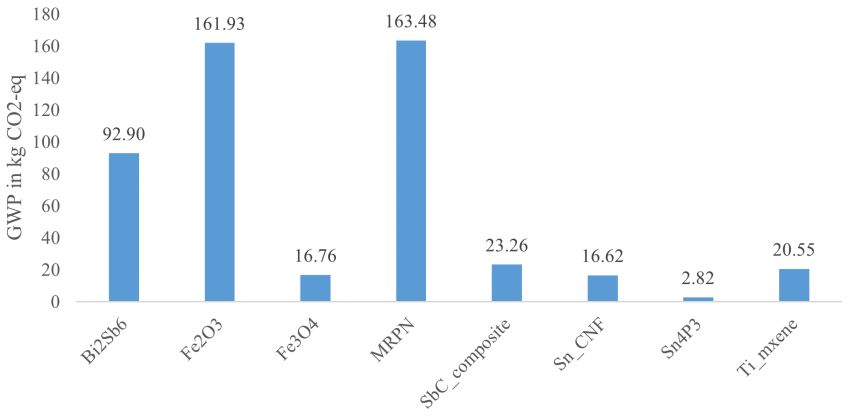

Figure 4.1: Comparison of Global Warming Potential of all anodes

In comparison with industrial-scale anode active material production based on Peters et al. (2021) [54], the emissions are significantly reduced to produce 1kg of active material, with a ratio of 1:3.5, demonstrating the economies of scale from laboratory to commercial-scale production expansion. Also, a detailed global warming potential is shown in the Figure 4.2.

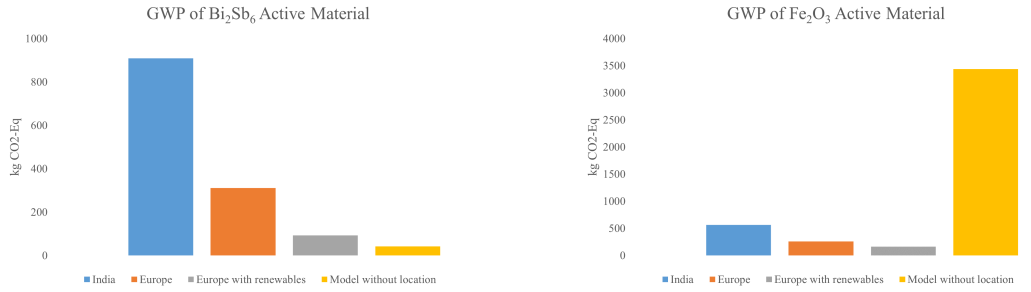

a. Global warming potential by Bi_2Sb_6 b. Global warming potential by Fe_2O_3

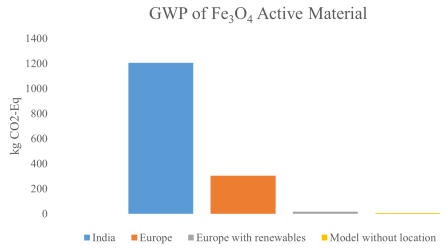

c. Global warming potential by Fe_3O_4

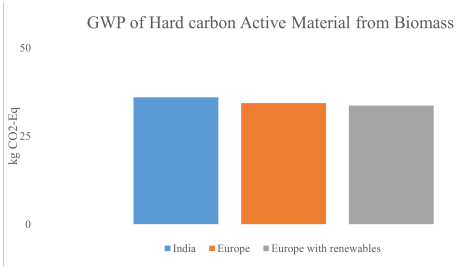

d. Global warming potential by Hard carbon from Biomass

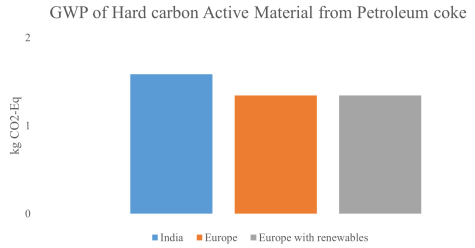

e. Global warming potential by Hard carbon from petroleum coke

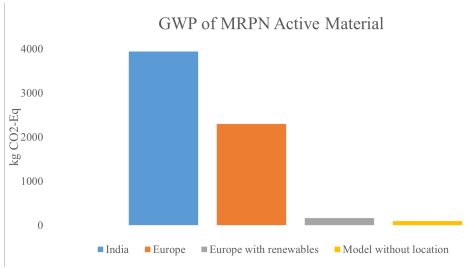

f. Global warming potential by Multi channel Red Phosphorous Nanotubes

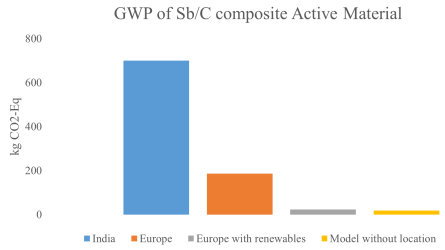

g. Global warming potential by SbC composite

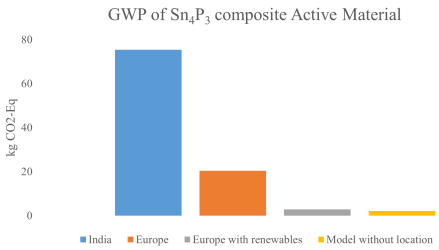

h. Global warming potential by Sn_4P_3

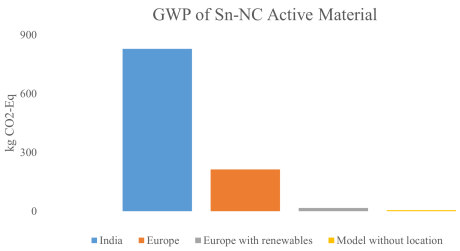

i. Global warming potential by Sn/CNF

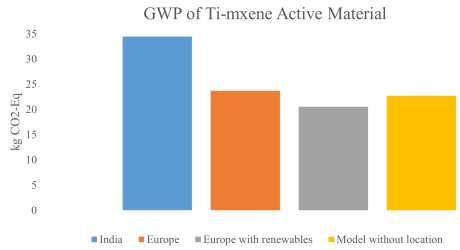

j. Global warming potential by Ti-mxene

Figure 4.2: Global warming potential of Anodes under different geographical locations

For abiotic depletion of resources, the conclusions between scenarios tended to be quite similar, with comparatively small variations between anode types as shown in the Figure 4.3. Even in this case, the electricity mix was found to be the major driver for differences by region, and the contribution from an individual precursor than in the case of GWP.

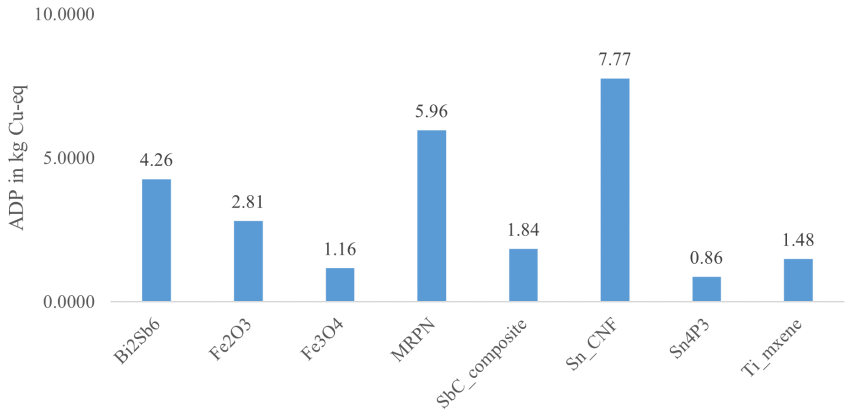

Figure 4.3: Comparison of Global Warming Potential of all anodes

In general, the research demonstrates that geographical location and synthesis pathway both bear effects on the environmental impact of emerging SIB anodes. While greener energy blends such as renewable-abundant European grids radically reduce GWP, process-specific considerations such as solvent choice and thermal power demands remain considerable hotspots worthy of attention in future optimisation studies.

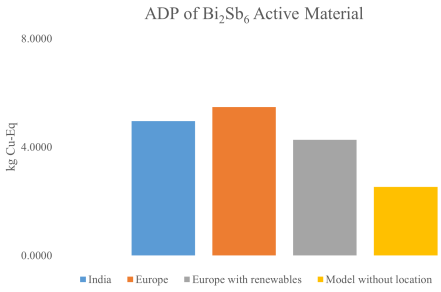

a. ADP by Bi_2Sb_6

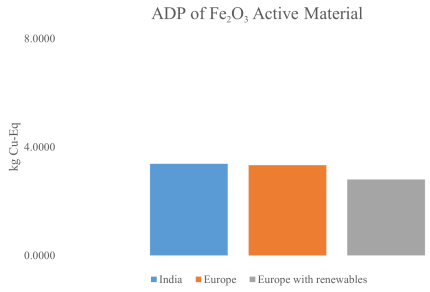

b. ADP by Fe_2O_3

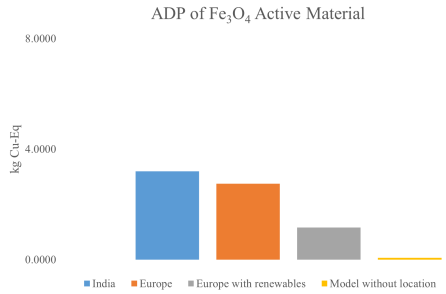

c. ADP by Fe_3O_4

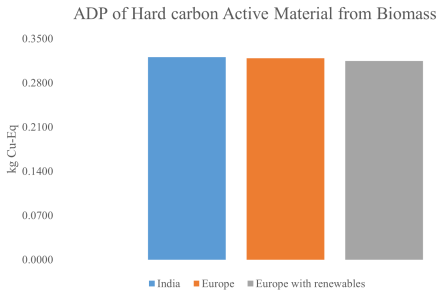

d. ADP by Hard carbon from Biomass

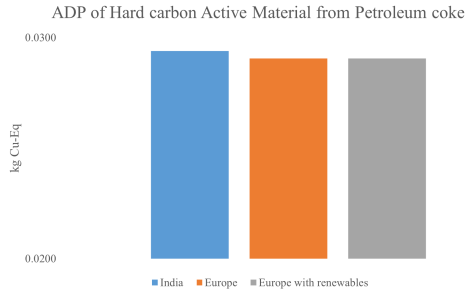

e. ADP by Hard carbon from petroleum coke

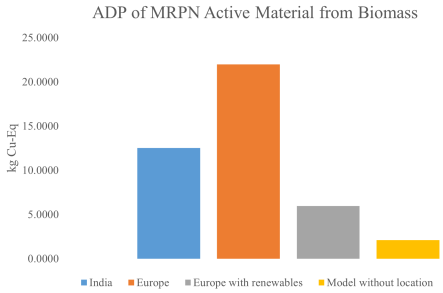

f. ADP by Multi channel Red Phosphorous Nanotubes

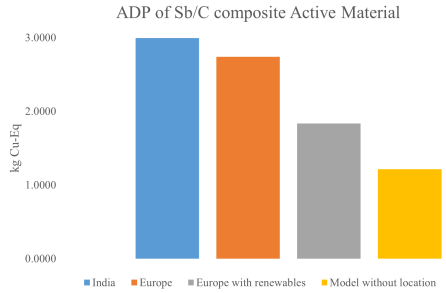

g. ADP by SbC composite

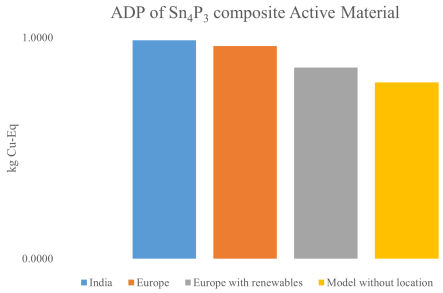

h. ADP by Sn_4P_3

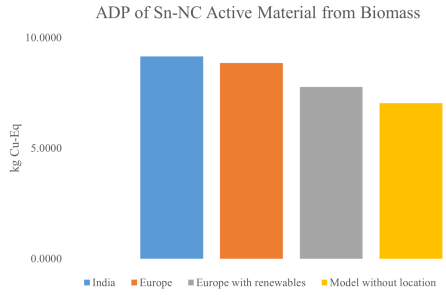

i. ADP by Sn/CNF

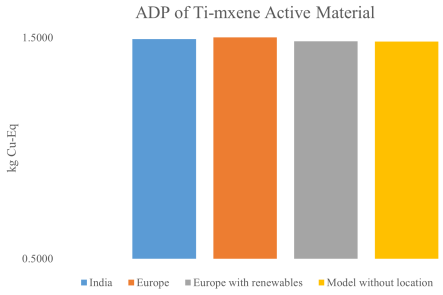

j. ADP by Ti-mxene

Figure 4.4: Abiotic Resource Depletion of Anodes under different locations

4.2 Observation on cathode and anode pairing

The selection of suitable cathode materials for each sodium-ion battery (SIB) anode is crucial and directly impacts the resulting cell's capacity, voltage, energy density, and cycle life. In this study, we analysed combinations for a range of anodes spanning metallic alloys, transition metal oxides, hard carbons, and advanced composites, matching each with proven and next-generation sodium-ion cathodes to maximise cell output and stability.

The pairing process for SIBs relies on aligning the voltage window and specific capacity of the anode with those of the cathode. The cathode should provide a stable and sufficiently high operating voltage (typically >2V vs Na/Na^+) and a robust capacity to ensure a balanced and efficient full cell. For example, $Na_3V_2(PO_4)_3$ a widely adopted polyanionic cathode offers a high and stable voltage plateau of 3.4 V and excellent cycling stability, making it favorable for high-capacity anodes such as Bi_2Sb_6, Fe_2O_3, Fe_3O_4, Sn_4P_3, and MXene materials. Prussian Blue Analogues (PBAs), with their open frameworks and multivalent redox, provide moderate-to-high voltage (3.2–3.3 V) and outstanding Na^+ mobility, allowing for rapid charge/discharge, which is ideal for both hard carbon and alloying-type anodes (e.g., SbC, Sn@NC). Layered oxides cathodes are also viable, offering voltages around 3 V and high capacities for full cells with oxide and alloy anodes, as well as for novel phosphorus and carbon-based anodes.

Matching anode and cathode not only ensures a suitable operating cell voltage but also manages

- The overlap of their reversible capacity windows
- Minimises irreversible capacity loss (especially important with conversion or alloying anodes)
- Delivers a balanced energy/power density. For example, hard carbon paired with PBAs yields cells with energy densities competitive with commercial lithium-ion technology, while maintaining safer and more sustainable chemistry.

The probable anode-cathode combinations are shown in the Table 3.1

Table 4.1: Anode-Cathode Combinations

Anode	**Cathode 1**	**Cathode 2**	**Cathode 3**	**Sources**
Bi_2Sb_6	$Na_3V_2(PO_4)_3$	Prussian Blue Analogues	–	[89]
Fe_2O_3	Layered oxide	–	–	
Fe_3O_4	Layered Oxide	–	–	[90]
HC_Biomass	Prussian Blue Analogues	$Na_3V_2(PO_4)_3$	$Na_{0.44}MnO_2$	[91][30]
HC_Pet Coke	Prussian Blue Analogues	Layered Oxide	Polyanionic	[91][30]
MRPN	Layered Oxides	Prussian Blue Analogues	–	[62]
SbC_composite	$Na_3V_2(PO_4)_3$	Prussian Blue Analogues	–	[92]
Sn@CNF	$Na_0.66MnO_2Na$	–	–	[61]
Sn_4P_3	$Na_3V_2(PO_4)_3$	–	–	[93]
Ti_mxene	$Na_3V_2(PO_4)_3$	Mxene based cathodes		[50]

Chapter 5

Conclusion and Future Scope

Conclusion

Sodium-ion batteries are also gaining increased interest as an alternative to lithium-ion systems. Though several cathode chemistries are being explored and developed, the majority of sodium-ion cells still rely on carbon-based anodes. Anode material research has picked up significantly in the last few years, though, offering new avenues for the improvement of battery performance.

This study contributes to the science community in designing and analysing an inventory database of sodium-ion battery materials. The database not only enables more thoughtful design of batteries and selection of materials but also enables life cycle assessment (LCA) of different cathode–anode combinations. Although this study focused on only two impact categories, this methodology can be extended to other more environmental indicators and will provide more insights when applied to full battery systems.

The LCA results demonstrate that energy consumption is the dominant driver of environmental impacts, and the role of fossil fuel inputs to the energy system is especially important. The mineral inputs critical to these technologies also contribute to higher emissions. Furthermore, electrochemical properties are also a critical factor: compounds with lower energy density in the anode require additional active material to supply the same amount of energy, which equates to greater material requirements and manufacturing energy consumption. These findings highlight that sodium-ion batteries, especially with optimised anodes, carry a great deal of environmental value if further optimised.

Limitation of the research

As with many early-stage studies, this research also possessed several limitations. The most pressing one was the unavailability of full inventory data. Certain precursors and intermediate products were missing in the LCA databases, so cautious estimations and modelling assumptions had to be used. This introduces a certain degree of uncertainty into the result. Another limitation is the unavailability of primary industrial data. Since most of the sodium-ion chemistries are still in the development phase, industry players keep process information secret. Therefore, this study had to rely predominantly on research reports and pilot-scale publications, which may not reflect actual industrial conditions accurately.

Furthermore, the scope of this thesis was limited to the stage of lab-scale synthesis of active materials. While this provides a necessary foundation, it doesn't account for the use-related impacts, charging cycles, or end-of-life processing such as recycling and material recovery. Such stages should alter the global life cycle profile of sodium-ion batteries, especially given that recycling approaches should significantly reduce the need for primary raw materials. Extending the scope to the whole life cycle would therefore provide a more realistic and holistic vision of the sustainability potential of SIBs.

Future Work

This study is the first step toward creating an anode active material inventory for sodium-ion batteries. The database must be updated and maintained regularly to be reliable and accurate. Data are primarily derived from literature reporting and calculation-based data, it is a starting point but with limited information on industrial processes. As the technology continues to develop, future updates should incorporate first-hand data from the industry, as well as improved methodologies described in research studies.

Apart from updates, the scope of the dataset will need to expand. Though this thesis focused on anode active materials, subsequent studies can include cathodes, electrolytes, binders, separators, and current collectors and eventually allow for full cell-level and system-level assessments. Expanded coverage like this would allow for greater LCAs and better comparisons between battery designs.

Finally, accessibility improvements will be required. The current Excel format is easy to use with small datasets but limiting for bigger inventories. A more user-friendly interface with searching ability, efficient data retrieval, and exportability to LCA packages would be time-efficient, error-reducing, and user-dataset friendly.

Creating such a collaborative environment in which researchers and industry partners can utilise data has the potential to make the dataset a robust, and community-maintained resource for sustainable battery development.

Appendix A

Anode Active Material Inventory List

Table A.1: Inventory List for Bi_2Sb_6 Active Material

Input Material	**Amount**	**Unit**
Antimony	1.2	g
Bismuth	0.6	g
Electricity	3.3	MJ
Heat	0.5	MJ
Magnesium	4.6	g
Output Material	**Amount**	**Unit**
np-Bi_2Sb_6 alloy (nanoporous), active material	1.7	g
Hydrogen, gaseous, low pressure	0.1	g
Magnesium (recovered)	4.6	g

Table A.2: Inventory List for Fe_2O_3 Active Material

Input Material	**Amount**	**Unit**
Tetraethyl orthosilicate	0.25	g
Iron acetate (precursor for Fe_2O_3)	2.25	g
Electricity	0.15	MJ
Heat	2.5	MJ
Acrylonitrile	6.5	g
Output Material	**Amount**	**Unit**
Fe_2O_3 active material	2.5	g

Table A.3: Inventory List for Fe_3O_4 Active Material

Input Material	**Amount**	**Unit**
$FeCl_3$ (Ferric chloride)	0.486	g
PVP (Polyvinylpyrrolidone)	0.6	g
DMF (N,N-Dimethylformamide)	10	ml
PAN (Polyacrylonitrile)	0.4	g
Electricity	0.35	MJ
Heat	2.5	MJ
Output Material	**Amount**	**Unit**
uf-Fe_3O_4@N-CNF membrane	0.9	g

Table A.4: Inventory List for Red Phosphorus (MRPN) Active Material

Input Material	**Amount**	**Unit**
PI_3 (Phosphorus Triiodide)	0.0823	g
Iodobenzene	5.18	g
CTAB (Cetyltrimethylammonium bromide)	0.0364	g
Ethylene Glycol	5.58	g
Electricity	0.1	MJ
Heat	2	MJ
Input Material	**Amount**	**Unit**
MRPN-3 Product	0.2	g
Solvent waste (iodobenzene, ethylene glycol)	10	g

Table A.5: Inventory List for Sb/C-Composite Active Material

Input Item	**Amount**	**Unit**
Sb_2O_3 powder	1.0	g
CaC_2 powder	1.0	g
Electricity	1.7	MJ
Heat	1.0	MJ
Input Material	**Amount**	**Unit**
Sb/C Composite	1.5	g

Table A.6: Inventory List for Sn_4P_3 Active Material

Input Material	**Amount**	**Unit**
Tin(II) chloride dihydrate	9.01	g
Red Phosphorus (CRP)	7.43	g
Reduced Graphene Oxide (rGO)	0.05	g
Electricity	0.3	MJ
Heat	2.5	MJ
Output Material	**Amount**	**Unit**
Sn_4P_3-rGO Composite (sample 2)	14.5	g

Table A.7: Inventory List for Sn/C-Nanofibers Active Material

Input Material	**Amount**	**Unit**
Carbon	0.12	g
Electricity	0.42	kWh
Tin	0.58	g
Output Material	**Amount**	**Unit**
Sn_NC active material	0.7	g

Table A.8: Inventory List for Ti MXene Active Material

Input Material	**Amount**	**Unit**
Titanium	10.31	g
Aluminium	5.81	g
Titanium carbide	23.9	g
Electricity	0.4	MJ
Output Material	**Amount**	**Unit**
$Ti_1Al_1TiC_{1.85}$ active material	40.9	g

Table A.9: Inventory List for Industrial Production of Hard Carbon Active Material from Biomass

Input Material	**Amount**	**Unit**
Carbohydrate	20	kg
Electricity	0.107	kWh
Heat	9.52	MJ
Water	0.178	l
Additives	0.267	kg
Inert atmosphere	6.99	kg
Transport, lorry	1.38	t·km
Transport, train	4.86	t·km
Infrastructure	4e-10	p
Dust	6.62e-05	kg
Output Material	**Amount**	**Unit**
CO_2	29.33	kg
CO	0.000353	kg
NO_x	0.00616	kg
SO_2	0.00117	kg
TOC	0.00011	kg
HF	8.89e-06	kg
HCl	0.000508	kg
Waste heat	9.9	MJ
Waste water	0.0178	l
Solid waste	0.000444	kg
Hard carbon	1	kg

Table A.10: Inventory List for Industrial Production of Hard Carbon Active Material from Petroleum Coke

Input Material	**Amount**	**Unit**
Coke	1.14	kg
Electricity	0.0183	kWh
Heat	1.89	MJ
Water	0.178	l
Inert atmosphere	0.9	kg
Transport, lorry	0.159	t·km
Transport, train	0.777	t·km
Infrastructure	4e-10	p
Output Material	**Amount**	**Unit**
CO_2	0.0839	kg
NO	0.0466	kg
NO_2	0.00376	kg
SO_2	0.0503	kg
Waste heat	1.95	MJ
Hard carbon	1	kg

Bibliography

[1] Dierk Raabe. «The Materials Science behind Sustainable Metals and Alloys». In: *Chemical Reviews* 123.5 (Mar. 2023), pp. 2436–2608. ISSN: 15206890. DOI: 10.1021/ACS.CHEMREV.2C00799. URL: /doi/pdf/10.1021/acs.chemrev.2c00799?ref=article_openPDF (cit. on p. 1).

[2] Sadnan Sakib, Md Biplob Hossain, Muhammad Ahsan Zamee, M. J. Hossain, and Md Ahasan Habib. «Role of battery energy storage systems: A comprehensive review on renewable energy zones integration in weak transmission networks». In: *Journal of Energy Storage* 128 (Aug. 2025), p. 117223. ISSN: 2352-152X. DOI: 10.1016/J.EST.2025.117223. URL: https://www.sciencedirect.com/science/article/pii/S2352152X2501936X (cit. on pp. 1, 2).

[3] Eduard Enasel and Gheorghe Dumitrascu. «Storage solutions for renewable energy: A review». In: *Energy Nexus* 17 (Mar. 2025), p. 100391. ISSN: 2772-4271. DOI: 10.1016/J.NEXUS.2025.100391. URL: https://www.sciencedirect.com/science/article/pii/S2772427125000324 (cit. on p. 1).

[4] International Renewable Energy Agency. «ELECTRICITY STORAGE AND RENEWABLES: COSTS AND MARKETS TO 2030 ELECTRICITY STORAGE AND RENEWABLES: COSTS AND MARKETS TO 2030 About IRENA». In: (2017). URL: www.irena.org (cit. on p. 1).

[5] Jang-Yeon Hwang, Yang-Kook Sun, and Seung-Taek Myung. *Sodium-ion batteries: present and future - Chemical Society Reviews*. English. 2017. DOI: https://doi.org/10.1039/C6CS00776G. URL: https://pubs.rsc.org/en/content/articlehtml/2017/cs/c6cs00776g (cit. on p. 1).

[6] Jennifer Cuahutencos. «Assessing the Opportunities and Risks of Extraction in the Lithium Assessing the Opportunities and Risks of Extraction in the Lithium Triangle Triangle». English. PhD thesis. Apr. 2024. URL: https://scholarship.claremont.edu/cmc_theses (cit. on p. 1).

[7] Walter Fernando Díaz Paz, Melisa Escosteguy, Lucas Seghezzo, Marc Hufty, Eduardo Kruse, and Martín Alejandro Iribarnegaray. «Lithium mining, water resources, and socio-economic issues in northern Argentina: We are not all in the same boat». In: *Resources Policy* 81 (Mar. 2023), p. 103288. ISSN: 0301-4207. DOI: 10.1016/J.RESOURPOL.2022.103288. URL: https://www.sciencedirect.com/science/article/abs/pii/S0301420722007310 (cit. on p. 1).

[8] María L. Vera, Walter R. Torres, Claudia I. Galli, Alexandre Chagnes, and Victoria Flexer. «Environmental impact of direct lithium extraction from brines». In: *Nature Reviews Earth and Environment* 4.3 (Mar. 2023), pp. 149–165. ISSN: 2662138X. DOI: 10.1038/S43017-022-00387-5;SUBJMETA. URL: https://www.nature.com/articles/s43017-022-00387-5 (cit. on p. 1).

[9] Michael D. Slater, Donghan Kim, Eungje Lee, and Christopher S. Johnson. «Sodium-Ion Batteries». In: *Advanced Functional Materials* 23.8 (Feb. 2013), pp. 947–958. ISSN: 1616-3028. DOI: 10.1002/ADFM.201200691. URL: /doi/pdf/10.1002/adfm.201200691%20https://onlinelibrary.wiley.com/doi/abs/10.1002/adfm.201200691%20https://advanced.onlinelibrary.wiley.com/doi/10.1002/adfm.201200691 (cit. on p. 1).

[10] Chayambuka and Kudakwashe. «Modeling of Sodium-ion Batteries». English. PhD thesis. Technische Universiteit Eindhoven, Mar. 2022. URL: www.tue.nl/taverne (cit. on pp. 1, 2).

[11] Madalin. *Sodium-ion Batteries 2023-2033: Technology, Players, Markets, and Forecasts – Hafenstrom*. Apr. 2023. URL: https://hafenstrom.com/sodium-ion-batteries-2023-2033-technology-players-markets-and-forecasts/ (cit. on p. 2).

[12] Ricardo Gabbay Souza, Ana Mariele Domingues, Anna Spindlegger, Claudia Mair-Bauernfeind, and Florian Part. «Review of the current knowledge and identified gaps in assessing the social and environmental impacts of mining processes in the Lithium Triangle». In: *Sustainable Production and Consumption* 53 (Jan. 2025), pp. 40–63. ISSN: 2352-5509. DOI: 10.1016/J.SPC.2024.11.031. URL: https://www.sciencedirect.com/science/article/pii/S2352550924003439 (cit. on p. 2).

[13] Jannis Wesselkämper, Laureen Dahrendorf, Lukas Mauler, Simon Lux, and Stephan von Delft. «Towards circular battery supply chains: Strategies to reduce material demand and the impact on mining and recycling». In: *Resources Policy* 95 (Aug. 2024), p. 105160. ISSN: 0301-4207. DOI: 10.1016/J.RESOURPOL.2024.105160. URL: https://www.sciencedirect.com/science/article/pii/S0301420724005270 (cit. on p. 2).

[14] Lei Wang, Hualing Tian, Xiang Yao, Yanjun Cai, Ziwei Gao, and Zhi Su. «Research Progress and Modification Measures of Anode and Cathode Materials for Sodium-Ion Batteries». In: *ChemElectroChem* 11.1 (Jan. 2024), e202300414. ISSN: 2196-0216. DOI: 10.1002/CELC.202300414. URL: /doi/pdf/10.1002/celc.202300414%20https://onlinelibrary.wiley.com/doi/abs/10.1002/celc.202300414%20https://chemistry-europe.onlinelibrary.wiley.com/doi/10.1002/celc.202300414 (cit. on pp. 2, 16).

[15] Qixing Jia, Zeyuan Li, Hulong Ruan, Dawei Luo, Junjun Wang, Zhiyu Ding, and Lina Chen. «A Review of Carbon Anode Materials for Sodium-Ion Batteries: Key Materials, Sodium-Storage Mechanisms, Applications, and Large-Scale Design Principles». In: *Molecules* 29.18 (Sept. 2024), p. 4331. ISSN: 14203049. DOI: 10.3390/MOLECULES29184331. URL: https://pmc.ncbi.nlm.nih.gov/articles/PMC11433841/ (cit. on p. 2).

[16] Syed Ali Riza, Ri Gan Xu, Qi Liu, Muhammad Hassan, Qiang Yang, Dao Bin Mu, Li Li, Feng Wu, and Ren Jie Chen. «A review of anode materials for sodium ion batteries». In: *New Carbon Materials* 39.5 (Oct. 2024), pp. 743–769. ISSN: 1872-5805. DOI: 10.1016/S1872-5805(24)60886-3. URL: https://www.sciencedirect.com/science/article/abs/pii/S1872580524608863 (cit. on pp. 2, 3).

[17] REBECCA NIBELIUS. «Life cycle assessment on sodium-ion cells for energy storage systems A cradle-to-gate study including 16 environmental perspectives, focusing on climate change impact». English. PhD thesis. KTH Royal Institute of Technology, 2023. URL: https://www.diva-portal.org/smash/get/diva2:1790721/FULLTEXT01.pdf (cit. on pp. 3, 4).

[18] Yujie Guo, Shun Ji, Feng Liu, Ziyi Zhu, Jie Xiao, Ke Liu, Yanjia Zhang, Shijun Liao, and Xiaoyuan Zeng. «A review of the preparation and characterization techniques for closed pores in hard carbon and their functions in sodium-ion batteries». In: *Energy Mater. 2025, 5, 500030.* 5.3 (Jan. 2025), N/A–N/A. ISSN: ISSN 2770-5900 (Online). DOI: 10.20517/ENERGYMATER.2024.63. URL: https://www.oaepublish.com/articles/energymater.2024.63 (cit. on p. 3).

[19] Yonas Tesfamhret, Marco Carboni, Desta Asfaw, Jolla Kullgren, and Reza Younesi. «Revealing capacity fading in Sb-based anodes using symmetric sodium-ion cells». In: *J. Phys. Mater* 4 (2021), p. 24007. DOI: 10.1088/2515-7639/abebe9. URL: https://doi.org/10.1088/2515-7639/abebe9 (cit. on p. 3).

[20] Bingying Pei, Haiqing Yu, Lei Zhang, Guozhao Fang, Jiang Zhou, Xinxin Cao, and Shuquan Liang. «Hard Carbon for Sodium-Ion Batteries: From Fundamental Research to Practical Applications». In: *Advanced Materials* (2025), p. 2504574. ISSN: 1521-4095. DOI: 10.1002/ADMA.202504574. URL: /doi/pdf/10.1002/adma.202504574%20https://onlinelibrary.wiley.com/doi/abs/10.1002/adma.202504574%20https://advanced.onlinelibrary.wiley.com/doi/10.1002/adma.202504574 (cit. on p. 3).

[21] Ryosuke Yokoi, Riki Kataoka, Titus Masese, Vanessa Bach, Matthias Finkbeiner, Marcel Weil, Manuel Baumann, and Masaharu Motoshita. «Potentials and hotspots of post-lithium-ion batteries: Environmental impacts and supply risks for sodium- and potassium-ion batteries». In: *Resources, Conservation and Recycling* 204 (May 2024), p. 107526. ISSN: 0921-3449. DOI: 10.1016/J.RESCONREC.2024.107526. URL: https://www.sciencedirect.com/science/article/pii/S0921344924001216 (cit. on p. 3).

[22] Bao Yi Mu et al. «A review of hard carbon anodes for rechargeable sodium-ion batteries». In: *New Carbon Materials* 39.5 (Oct. 2024), pp. 796–823. ISSN: 1872-5805. DOI: 10.1016/S1872-5805(24)60884-X. URL: https://www.sciencedirect.com/science/article/abs/pii/S187258052460884X (cit. on p. 3).

[23] Jens Peters, Daniel Buchholz, Stefano Passerini, and Marcel Weil. «Life cycle assessment of sodium-ion batteries». In: *Energy & Environmental Science* 9.5 (May 2016), pp. 1744–1751. ISSN: 1754-5706. DOI: 10.1039/C6EE00640J. URL: https://pubs.rsc.org/en/content/articlehtml/2016/ee/c6ee00640j%20https://pubs.rsc.org/en/content/articlelanding/2016/ee/c6ee00640j (cit. on pp. 3, 11, 13, 16, 17).

[24] Sanna Wickerts, Rickard Arvidsson, Anders Nordelöf, Magdalena Svanström, and Patrik Johansson. «Prospective life cycle assessment of sodium-ion batteries made from abundant elements». In: *Journal of Industrial Ecology* 28.1 (Feb. 2024), pp. 116–129. ISSN: 1530-9290. DOI: 10.1111/JIEC.13452. URL: /doi/pdf/10.1111/jiec.13452%20https://onlinelibrary.wiley.com/doi/abs/10.1111/jiec.13452%20https://onlinelibrary.wiley.com/doi/10.1111/jiec.13452 (cit. on pp. 3, 4, 6, 12, 14, 17).

[25] Shan Zhang, Bernhard Steubing, Hanna Karlsson Potter, Per Anders Hansson, and Åke Nordberg. «Future climate impacts of sodium-ion batteries». In: *Resources, Conservation and Recycling* 202 (Mar. 2024), p. 107362. ISSN: 0921-3449. DOI: 10.1016/J.RESCONREC.2023.107362. URL: https://www.sciencedirect.com/science/article/pii/S0921344923004962 (cit. on p. 3).

[26] Xue Bai, Nannan Wu, Gengchen Yu, and Tao Li. «Recent Advances in Anode Materials for Sodium-Ion Batteries». In: *Inorganics 2023, Vol. 11, Page 289* 11.7 (July 2023), p. 289. ISSN: 2304-6740. DOI: 10.3390/INORGANICS11070289. URL: https://www.mdpi.com/2304-6740/11/7/289/htm%20https://www.mdpi.com/2304-6740/11/7/289 (cit. on p. 3).

[27] Peeyush Phogat, Subhadeepa Dey, and Meher Wan. «Comprehensive review of Sodium-Ion Batteries: Principles, Materials, Performance, Challenges, and future Perspectives». In: *Materials Science and Engineering: B* 312 (Feb. 2025), p. 117870. ISSN: 0921-5107. DOI: 10.1016/J.MSEB.2024.117870. URL: https://www.sciencedirect.com/science/article/abs/pii/S0921510724006998 (cit. on p. 4).

[28] Gamzenur Özsin. «An overview of sodium-ion batteries as next-generation sustainable electrochemicaldevices beyond the traditional lithium-ion framework». In: *Turkish Journal of Chemistry* 49.1 (Feb. 2025), pp. 1–28. ISSN: 1300-0527. DOI: 10.55730/1300-0527.3707. URL: https://journals.tubitak.gov.tr/chem/vol49/iss1/2 (cit. on pp. 5, 6).

[29] Nanthini Mohana Suntharam, Shahid Bashir, Vengadaesvaran B, Nasrudin Abd Rahim, Reasmyraj S, S. Ramesh, K. Ramesh, and Thibeorchews Prasankumar. «Fundamentals and key components of sodium-ion batteries: Challenges and future perspectives». In: *Materials Today Chemistry* 42 (Dec. 2024), p. 102350. ISSN: 2468-5194. DOI: 10.1016/J.MTCHEM.2024.102350. URL: https://www.sciencedirect.com/science/article/pii/S2468519424004567 (cit. on pp. 5, 6).

[30] Yun Gao, Hang Zhang, Jian Peng, Lin Li, Yao Xiao, Li Li, Yang Liu, Yun Qiao, and Shu Lei Chou. «A 30-year overview of sodium-ion batteries». In: *Carbon Energy* 6.6 (June 2024), e464. ISSN: 2637-9368. DOI: 10.1002/CEY2.464. URL: /doi/pdf/10.1002/cey2.464%20https://onlinelibrary.wiley.com/doi/abs/10.1002/cey2.464%20https://onlinelibrary.wiley.com/doi/10.1002/cey2.464 (cit. on pp. 5, 37).

[31] AtomFair. *Fundamentals of Sodium-Ion Battery Chemistry*. 2025. URL: https://atomfair.com/battery-equipment-and-instrument/article.php?id=G79-1505 (cit. on p. 6).

[32] Han Zhang, Liguang Wang, and Pengjian Zuo. «Advances in sodium-ion battery cathode materials: exploring chemistry, reaction mechanisms, and prospects for next-generation energy storage systems». In: *Journal of Materials Chemistry A* 12.45 (Nov. 2024), pp. 30971–31003. ISSN: 2050-7496. DOI: 10.1039/D4TA03748K. URL: https://pubs.rsc.org/en/content/articlehtml/2024/ta/d4ta03748k%20https://pubs.rsc.org/en/content/articlelanding/2024/ta/d4ta03748k (cit. on p. 6).

[33] Sam Krampf. *What's Currently Happening in Sodium-Ion Batteries? 2025*. English. Apr. 2025. URL: https://sodiumbatteryhub.com/2025/04/10/whats-currently-happening-in-sodium-ion-batteries-2025/ (cit. on p. 7).

[34] Nikhil Kaitwade. *Energy Storage Sodium Ion Battery Market | Global Market Analysis Report - 2035*. English. 2024. URL: https://www.futuremarketinsights.com/reports/energy-storage-sodium-ion-battery-market (cit. on p. 7).

[35] The Battery Show Asia. *Sodium-Ion Battery Technology Breakthroughs in China Are Driving the Energy Future - The Battery Show Asia*. Mar. 2025. URL: https://www.thebatteryshow.asia/sodium-ion-battery-technology-breakthroughs-in-china-are-driving-the-energy-future/ (cit. on p. 7).

[36] Christopher Chico. *Beyond Lithium: Unveiling the Promise of Sodium-Ion Batteries*. English. Mar. 2025. URL: https://christopherchico.substack.com/p/beyond-lithium-unveiling-the-promise (cit. on p. 7).

[37] IDTechEx. *Sodium-ion Batteries 2025-2035: Technology, Players, Markets, and Forecasts*. 2025. URL: https://www.idtechex.com/en/research-report/sodium-ion-batteries-2025-2035-technology-players-markets-and-forecasts/1082 (cit. on p. 7).

[38] Shuangyan Qiao, Qianwen Zhou, Meng Ma, Hua Kun Liu, Shi Xue Dou, and Shaokun Chong. «Advanced Anode Materials for Rechargeable Sodium-Ion Batteries». In: *ACS nano* 17.12 (June 2023), pp. 11220–11252. ISSN: 1936-086X. DOI: 10.1021/ACSNANO.3C02892. URL: https://pubmed.ncbi.nlm.nih.gov/37289640/ (cit. on p. 8).

[39] Ziyang Lu et al. «Consummating ion desolvation in hard carbon anodes for reversible sodium storage». In: *Nature Communications* 15.1 (Dec. 2024), pp. 1–13. ISSN: 20411723. DOI: 10.1038/S41467-024-47522-Y;TECHMETA. URL: https://www.nature.com/articles/s41467-024-47522-y (cit. on p. 8).

[40] Chun Wu, Yunrui Yang, Yinghao Zhang, Hui Xu, Xiangxi He, Xingqiao Wu, and Shulei Chou. «Hard carbon for sodium-ion batteries: progress, strategies and future perspective». In: *Chemical Science* 15.17 (May 2024), pp. 6244–6268. ISSN: 2041-6539. DOI: 10.1039/D4SC00734D. URL: https://pubs.rsc.org/en/content/articlehtml/2024/sc/d4sc00734d%20https://pubs.rsc.org/en/content/articlelanding/2024/sc/d4sc00734d (cit. on p. 8).

[41] Farah Nabilah Shafiee, Siti Aminah Mohd Noor, Muhammad Amirul Aizat Mohd Abdah, Siti Hasnawati Jamal, and Alinda Samsuri. «Recent progress on hard carbon and other anode materials for sodium-ion batteries». In: *Heliyon* 10.8 (Apr. 2024), e29512. ISSN: 24058440. DOI: 10.1016/J.HELIYON.2024.E29512. URL: https://pmc.ncbi.nlm.nih.gov/articles/PMC11063408/ (cit. on p. 8).

[42] Amalie Skurtveit, Anders Brennhagen, Heesoo Park, Carmen Cavallo, and Alexey Y. Koposov. «Benefits and Development Challenges for Conversion-Alloying Anode Materials in Na-Ion Batteries». In: *Frontiers in Energy Research* 10 (Apr. 2022), p. 897755. ISSN: 2296598X. DOI: 10.3389/FENRG.2022.897755/BIBTEX. URL: www.frontiersin.org (cit. on pp. 8, 9).

[43] Ata-ur Rehman, Sanum Saleem, Shahid Ali, Syed Mustansar Abbas, Minsu Choi, and Wonchang Choi. «Recent advances in alloying anode materials for sodium-ion batteries: material design and prospects». In: *Energy Mater 2024;4:400068.* 4.6 (July 2024), N/A–N/A. ISSN: ISSN 2770-5900 (Online). DOI: 10.20517/ENERGYMATER.2024.06. URL: https://www.oaepublish.com/articles/energymater.2024.06 (cit. on pp. 8, 10).

[44] Zhaolin Li and Hailei Zhao. «Recent developments of phosphorus-based anodes for sodium ion batteries». In: *Journal of Materials Chemistry A* 6.47 (Dec. 2018), pp. 24013–24030. ISSN: 2050-7496. DOI: 10.1039/C8TA08774A. URL: https://pubs.rsc.org/en/content/articlehtml/2018/ta/c8ta08774a%20https://pubs.rsc.org/en/content/articlelanding/2018/ta/c8ta08774a (cit. on p. 8).

[45] Hiroki Kotaka, Hiroyoshi Momida, and Tamio Oguchi. «Performance and reaction mechanisms of tin compounds as high-capacity negative electrodes of lithium and sodium ion batteries». In: *Materials Advances* 3.6 (Mar. 2022), pp. 2793–2799. ISSN: 26335409. DOI: 10.1039/D1MA00967B. URL: https://pubs.rsc.org/en/content/articlehtml/2022/ma/d1ma00967b%20https://pubs.rsc.org/en/content/articlelanding/2022/ma/d1ma00967b (cit. on p. 8).

[46] Tasnuva Sharmin, Nazmul Hossain, Fatima Tasneem Mohsin, Md Azazul Haque, Mohammad Muhtasim Mashfy, Tamzeed Ahmed Alvy, and Mohammad Nasim. «Advancements in cutting-edge materials for sodium-ion battery anodes: A comprehensive review». In: *Materials Today Chemistry* 42 (Dec. 2024), p. 102407. ISSN: 2468-5194. DOI: 10.1016/J.MTCHEM.2024.102407. URL: https://www.sciencedirect.com/science/article/pii/S2468519424005135 (cit. on pp. 9, 16, 20).

[47] Lantao Liu, Qian Xu, Songhe Yin, Zishuai Liu, Yongfeng Li, and Weiwei Pang. «Recent progress on hard carbon-based anode for sodium-ion battery». In: *Journal of Power Sources* 615 (Sept. 2024), p. 235116. ISSN: 0378-7753. DOI: 10.1016/J.JPOWSOUR.2024.235116. URL: https://www.sciencedirect.com/science/article/abs/pii/S0378775324010681 (cit. on p. 8).

[48] Yanhua Wan, Yao Liu, Dongliang Chao, Wei Li, and Dongyuan Zhao. «Recent advances in hard carbon anodes with high initial Coulombic efficiency for sodium-ion batteries». In: *Nano Materials Science* 5.2 (June 2023), pp. 189–201. ISSN: 2589-9651. DOI: 10.1016/J.NANOMS.2022.02.001. URL: https://www.sciencedirect.com/science/article/pii/S2589965122000058 (cit. on p. 8).

[49] Zheng Guang Liu, Jiahua Zhao, Hao Yao, Xiang Xi He, Hang Zhang, Yun Qiao, Xing Qiao Wu, Li Li, and Shu Lei Chou. «P-doped spherical hard carbon with high initial coulombic efficiency and enhanced capacity for sodium ion batteries». In: *Chemical Science* 15.22 (June 2024), pp. 8478–8487. ISSN: 2041-6539. DOI: 10.1039/D4SC01395F. URL: https://pubs.rsc.org/en/content/articlehtml/2024/sc/d4sc01395f%20https://pubs.rsc.org/en/content/articlelanding/2024/sc/d4sc01395f (cit. on p. 9).

[50] Wenchao Bi, Shuo Li, Wenshun Wang, Yuan Liu, Jun Shen, Guohua Gao, Zenghai Zhang, Guangming Wu, and Guozhong Cao. «MXenes and their composites as electrodes for sodium ion batteries». In: *Energy Storage Materials* 71 (Aug. 2024), p. 103568. ISSN: 2405-8297. DOI: 10.1016/J.ENSM.2024.103568. URL: https://www.sciencedirect.com/science/article/abs/pii/S2405829724003945 (cit. on pp. 9, 26, 27, 37).

[51] Zheng Yi, Daliang Fang, Wanqun Zhang, Jie Tian, Shimou Chen, Jianbo Liang, Ning Lin, and Yitai Qian. «Revealing Quasi-1D Volume Expansion in Na-/K-Ion Battery Anodes: A Case Study of Sb2O3 Microbelts». In: *CCS Chemistry* 3.5 (May 2021), pp. 1306–1315. ISSN: 20965745. DOI: 10.31635/CCSCHEM.020.202000321. URL: /doi/pdf/10.31635/ccschem.020.202000321 (cit. on p. 10).

[52] Jian-Jia Mu, Zhao-Meng Liu, Qing-Song Lai, Da Wang, Xuan-Wen Gao, Dong-Run Yang, Hong Chen, and Wen-Bin Luo. «An industrial pathway to emerging presodiation strategies for increasing the reversible ions in sodium-ion batteries and capacitors». In: *Energy Mater 2022;2:200043.* 2.6 (Dec. 2022), N/A–N/A. ISSN: ISSN 2770-5900 (Online). DOI: 10.20517/ENERGYMATER.2022.57. URL: https://www.oaepublish.com/articles/energymater.2022.57 (cit. on p. 10).

[53] Yuxin Liu. «Techno-economic Analysis of Biomass Conversion to Hard Carbon Materials». English. In: (2022). URL: https://urn.kb.se/resolve?urn=urn:nbn:se:kth:diva-315050 (cit. on p. 10).

[54] Jans Peters, Manuel Baumann, Joachim Binder, and Marcel Well. «On the environmental competitiveness of sodium-ion batteries under a full life cycle perspective – a cell-chemistry specific modelling approach - Sustainable Energy & Fuels». In: *Sustainable Energy Fuels* 5 (Nov. 2021), pp. 6414–6429. DOI: 10.1039/d1se01292d. URL: https://pubs.rsc.org/en/content/articlehtml/2021/se/d1se01292d (cit. on pp. 11, 13, 16, 17, 27, 30, 32).

[55] Simon F. Schneider, Christian Bauer, Petr Novák, and Erik J. Berg. «A modeling framework to assess specific energy, costs and environmental impacts of Li-ion and Na-ion batteries». In: *Sustainable Energy & Fuels* 3.11 (Oct. 2019), pp. 3061–3070. ISSN: 2398-4902. DOI: 10.1039/C9SE00427K. URL: https://pubs.rsc.org/en/content/articlehtml/2019/se/c9se00427k%20https://pubs.rsc.org/en/content/articlelanding/2019/se/c9se00427k (cit. on pp. 11, 17).

[56] Haoyu Liu, Zhen Xu, Zhenyu Guo, Jingyu Feng, Haoran Li, Tong Qiu, and Magdalena Titirici. «A life cycle assessment of hard carbon anodes for sodium-ion batteries». In: *Philosophical transactions. Series A, Mathematical, physical, and engineering sciences* 379.2209 (Nov. 2021). ISSN: 1471-2962. DOI: 10.1098/RSTA.2020.0340. URL: https://pubmed.ncbi.nlm.nih.gov/34510922/ (cit. on pp. 12, 14, 23).

[57] Carlos Felgueiras et al. «LCA and C-LCC Indicator as Tools for Sodium-Ion Batteries' Eco-Design». In: (2023). DOI: 10.3390/en16176220. URL: https://doi.org/10.3390/en16176220 (cit. on pp. 12, 17).

[58] Jens F. Peters, Mohammad Abdelbaky, Manuel Baumann, and Marcel Weil. «A review of hard carbon anode materials for sodium-ion batteries and their environmental assessment». In: *Matériaux & Techniques* 107.5 (2019), p. 503. ISSN: 0032-6895. DOI: 10.1051/MATTECH/2019029. URL: https://www.mattech-journal.org/articles/mattech/full_html/2019/05/mt190046/mt190046.html%20https://www.mattech-journal.org/articles/mattech/abs/2019/05/mt190046/mt190046.html (cit. on p. 13).

[59] Angela Malara, Fabiola Pantò, Saveria Santangelo, Pier Luigi Antonucci, Michele Fiore, Gianluca Longoni, Riccardo Ruffo, and Patrizia Frontera. «Comparative life cycle assessment of Fe2O3-based fibers as anode materials for sodium-ion batteries». In: *Environment, Development and Sustainability* 23.5 (May 2021), pp. 6786–6799. ISSN: 15732975. DOI: 10.1007/S10668-020-00891-Y/FIGURES/7. URL: https://link.springer.com/article/10.1007/s10668-020-00891-y (cit. on pp. 13, 17, 20).

[60] Fatemeh Mozaffarpour, Nafiseh Hassanzadeh, and Ehsan Vahidi. «Comparative life cycle assessment of synthesis routes for cathode materials in sodium-ion batteries». In: *Clean Technologies and Environmental Policy* 24.10 (Dec. 2022), pp. 3319–3330. ISSN: 16189558. DOI: 10.1007/S10098-022-02381-3/FIGURES/6. URL: https://link.springer.com/article/10.1007/s10098-022-02381-3 (cit. on p. 14).

[61] Maria Leonor Carvalho, Giulio Mela, Andrea Temporelli, Elisabetta Brivio, and Pierpaolo Girardi. «Sodium-Ion Batteries with Ti1 Al1 TiC1.85 MXene as Negative Electrode: Life Cycle Assessment and Life Critical Resource Use Analysis». In: *Sustainability (Switzerland)* 14.10 (May 2022), p. 5976. ISSN: 20711050. DOI: 10.3390/SU14105976/S1. URL: https://www.mdpi.com/2071-1050/14/10/5976/htm%20https://www.mdpi.com/2071-1050/14/10/5976 (cit. on pp. 14, 20, 23, 25, 37).

[62] Santanu Mukherjee, Shakir Bin Mujib, Davi Soares, and Gurpreet Singh. «Electrode Materials for High-Performance Sodium-Ion Batteries». In: *Materials* 12.12 (June 2019), p. 1952. ISSN: 19961944. DOI: 10.3390/MA12121952. URL: https://pmc.ncbi.nlm.nih.gov/articles/PMC6630545/ (cit. on pp. 16, 37).

[63] Zhaoguo Liu, Ziyang Lu, Shaohua Guo, Quan Hong Yang, and Haoshen Zhou. «Toward High Performance Anodes for Sodium-Ion Batteries: From Hard Carbons to Anode-Free Systems». In: *ACS Central Science* 9.6 (June 2023), pp. 1076–1087. ISSN: 23747951. DOI: 10.1021/ACSCENTSCI.3C00301. URL: /doi/pdf/10.1021/acscentsci.3c00301?ref=article_openPDF (cit. on p. 16).

[64] Akiko Tsurumaki, Sergio Brutti, and Maria Assunta Navarra. «Closed Battery Systems». In: *Emerging Battery Technologies to Boost the Clean Energy Transition*. Ed. by Stefano Passerin, Linda Barelli, Manuel Baumann, Jens Peters, and Marcel Weil. Materials Research Society, 2024, pp. 173–212. URL: https://link.springer.com/book/10.1007/978-3-031-48359-2 (cit. on p. 17).

[65] Michele Fiore, Gianluca Longoni, Saveria Santangelo, Fabiola Pantò, Sara Stelitano, Patrizia Frontera, Pierluigi Antonucci, and Riccardo Ruffo. «Electrochemical characterization of highly abundant, low cost iron (III) oxide as anode material for sodium-ion rechargeable batteries». In: *Electrochimica Acta* 269 (Apr. 2018), pp. 367–377. ISSN: 0013-4686. DOI: 10.1016/J.ELECTACTA.2018.02.161. URL: https://www.sciencedirect.com/science/article/pii/S0013468618304754#sec2 (cit. on pp. 17, 25).

[66] Hui Gao, Jiazheng Niu, Chi Zhang, Zhangquan Peng, and Zhonghua Zhang. «A Dealloying Synthetic Strategy for Nanoporous Bismuth–Antimony Anodes for Sodium Ion Batteries». In: *ACS Nano* 12.4 (Apr. 2018), pp. 3568–3577. ISSN: 1936086X. DOI: 10.1021/ACSNANO.8B00643. URL: https://pubs.acs.org/doi/abs/10.1021/acsnano.8b00643 (cit. on pp. 18, 20, 26).

[67] Yanqing Fu, Qiliang Wei, Gaixia Zhang, and Shuhui Sun. «Advanced Phosphorus‐Based Materials for Lithium/Sodium-Ion Batteries: Recent Developments and Future Perspectives». In: *Advanced Energy Materials* 8.13 (May 2018), p. 1703058. ISSN: 1614-6840. DOI: 10.1002/AENM.201702849. URL: /doi/pdf/10.1002/aenm.201702849%20https://onlinelibrary.wiley.com/doi/abs/10.1002/aenm.201702849%20https://advanced.onlinelibrary.wiley.com/doi/10.1002/aenm.201702849 (cit. on p. 18).

[68] Konstantina A. Papadopoulou, Alexander Chroneos, and Stavros Richard G. Christopoulos. «Latest advances and comparative analysis of MXenes as anode and cathode electrodes in secondary batteries». In: *Journal of Applied Physics* 133.3 (Jan. 2023), p. 30901. ISSN: 0021-8979. DOI: 10.1063/5.0136840. URL: /aip/jap/article/133/3/030901/2867595/Latest-advances-and-comparative-analysis-of-MXenes (cit. on p. 18).

[69] Esperanza Batuecas, Cynthia S. Martínez-Cisneros, Daniel Serrano, and Alejandro Várez. «Life cycle assessment of lab-scale solid sodium-ion batteries: A sustainable alternative to liquid lithium-ion batteries». In: *Journal of Energy Storage* 80 (Mar. 2024), p. 110355. ISSN: 2352-152X. DOI: 10.1016/J.EST.2023.110355. URL: https://www.sciencedirect.com/science/article/pii/S2352152X23037544 (cit. on p. 18).

[70] Florian Degen, Miriam Mitterfellner, and Achim Kampker. «Comparative life cycle assessment of lithium-ion, sodium-ion, and solid-state battery cells for electric vehicles». In: *Journal of Industrial Ecology* 29.1 (Feb. 2025), pp. 113–128. ISSN: 1530-9290. DOI: 10.1111/JIEC.13594. URL: /doi/pdf/10.1111/jiec.13594%20https://onlinelibrary.wiley.com/doi/abs/10.1111/jiec.13594%20https://onlinelibrary.wiley.com/doi/10.1111/jiec.13594 (cit. on p. 18).

[71] Lichuan Wang, Jolanta Świątowska, Sirui Dai, Minglei Cao, Zhicheng Zhong, Yan Shen, and Mingkui Wang. «Promises and challenges of alloy-type and conversion-type anode materials for sodium–ion batteries». In: *Materials Today Energy* 11 (Mar. 2019), pp. 46–60. ISSN: 2468-6069. DOI: 10.1016/J.MTENER.2018.10.017. URL: https://www.sciencedirect.com/science/article/abs/pii/S2468606918302491?via%3Dihub (cit. on p. 19).

[72] Yating Yuan, Safeer Jan, Zhiyong Wang, and Xianbo Jin. «A simple synthesis of nanoporous Sb/C with high Sb content and dispersity as an advanced anode for sodium ion batteries». In: *Journal of Materials Chemistry A* 6.14 (Apr. 2018), pp. 5555–5559. ISSN: 2050-7496. DOI: 10.1039/C8TA00592C. URL: https://pubs.rsc.org/en/content/articlehtml/2018/ta/c8ta00592c%20https://pubs.rsc.org/en/content/articlelanding/2018/ta/c8ta00592c (cit. on pp. 20, 24).

[73] Qingshan Zhao et al. «PVP-assisted synthesis of ultrafine transition metal oxides encapsulated in nitrogen-doped carbon nanofibers as robust and flexible anodes for sodium-ion batteries». In: *Carbon* 174 (Apr. 2021), pp. 325–334. ISSN: 0008-6223. DOI: 10.1016/J.CARBON.2020.12.016. URL: https://www.sciencedirect.com/science/article/pii/S0008622320311933?via%3Dihub#sec2 (cit. on p. 20).

[74] Palanisamy Santhoshkumar, Nitheesha Shaji, Murugan Nanthagopal, Jae Woo Park, Chenrayan Senthil, and Chang Woo Lee. «Multichannel red phosphorus with a nanoporous architecture: A novel anode material for sodium-ion batteries». In: *Journal of Power Sources* 470 (Sept. 2020), p. 228459. ISSN: 0378-7753. DOI: 10.1016/J.JPOWSOUR.2020.228459. URL: https://www.sciencedirect.com/science/article/pii/S0378775320307631#sec2 (cit. on pp. 20, 24).

[75] Site Li, Ziming Wang, Jun Liu, Linyu Yang, Yue Guo, Lizi Cheng, Ming Lei, and Wenjun Wang. «Yolk–Shell Sn@C Eggette-like Nanostructure: Application in Lithium-Ion and Sodium-Ion Batteries». In: *ACS Applied Materials and Interfaces* 8.30 (Aug. 2016), pp. 19438–19445. ISSN: 19448252. DOI: 10.1021/ACSAMI.6B04736. URL: https://pubs.acs.org/doi/abs/10.1021/acsami.6b04736 (cit. on p. 20).

[76] Weili Liu, Xianxia Yuan, and Xuebin Yu. «One-Step Solvothermal Route to Sn4P3-Reduced Graphene Oxide Nanohybrids as Cycle-Stable Anode Materials for Sodium-Ion Batteries». In: *ACS Applied Materials & Interfaces* 13.10 (Mar. 2021), pp. 12016–12024. ISSN: 19448252. DOI: 10.1021/ACSAMI.0C23052. URL: https://pubs.acs.org/doi/abs/10.1021/acsami.0c23052 (cit. on pp. 20, 24).

[77] Darío Alvira, Daniel Antorán, and Joan J. Manyà. «Plant-derived hard carbon as anode for sodium-ion batteries: A comprehensive review to guide interdisciplinary research». In: *Chemical Engineering Journal* 447 (Nov. 2022), p. 137468. ISSN: 1385-8947. DOI: 10.1016/J.CEJ.2022.137468. URL: https://www.sciencedirect.com/science/article/pii/S1385894722029564 (cit. on p. 23).

[78] Gaoyue Zhang, Chao Chen, Chenchen Xu, Junxiao Li, Hualin Ye, Ao Wang, Xin Cao, Kang Sun, and Jianchun Jiang. «Unraveling the Microcrystalline Carbon Evolution Mechanism of Biomass-Derived Hard Carbon for Sodium-Ion Batteries». In: *Energy & Fuels* 38.9 (May 2024), pp. 8326–8336. ISSN: 15205029. DOI: 10.1021/ACS.ENERGYFUELS.4C00823. URL: https://pubs.acs.org/doi/abs/10.1021/acs.energyfuels.4c00823 (cit. on p. 23).

[79] Palanivel Molaiyan, Glaydson Simões, Diwakar Karuppiah, Chandrasekar M Subramaniyam, Flaviano García-Alvarado, and Ulla Lassi. «Recent Progress in Biomass-Derived Carbon Materials for Li-Ion and Na-Ion Batteries-A Review». In: (2023). DOI: 10.3390/batteries9020116. URL: https://doi.org/10.3390/batteries9020116 (cit. on p. 23).

[80] Peng Zhou et al. «Synthesis and Electrochemical Performance of ZnSe Electrospinning Nanofibers as an Anode Material for Lithium Ion and Sodium Ion Batteries». In: *Frontiers in Chemistry* 7 (Aug. 2019), p. 473780. ISSN: 22962646. DOI: 10.3389/FCHEM.2019.00569/BIBTEX. URL: www.frontiersin.org (cit. on p. 25).

[81] Luchao Yue et al. «Recent advances in electrospun one-dimensional carbon nanofiber structures/heterostructures as anode materials for sodium ion batteries». In: *Journal of Materials Chemistry A* 8.23 (June 2020), pp. 11493–11510. ISSN: 2050-7496. DOI: 10.1039/D0TA03963B. URL: https://pubs.rsc.org/en/content/articlehtml/2020/ta/d0ta03963b%20https://pubs.rsc.org/en/content/articlelanding/2020/ta/d0ta03963b (cit. on p. 25).

[82] *India - Countries & Regions - IEA*. URL: https://www.iea.org/countries/india/energy-mix (cit. on pp. 28, 31).

[83] Marc-Andree WOLF, Kirana CHOMKHAMSRI, Miguel BRANDAO, Rana PANT, Fulvio ARDENTE, David PENNINGTON, Simone MANFREDI, CAMILLIS Camillo DE, and Malgorzata GORALCZYK. «International Reference Life Cycle Data System (ILCD) Handbook - General guide for Life Cycle Assessment - Detailed guidance». In: *Constraints* (2010), p. 417. ISSN: 1018-5593. DOI: 10.2788/38479. URL: https://publications.jrc.ec.europa.eu/repository/handle/JRC48157 (cit. on p. 28).

[84] Michael HAUSCHILD, Mark GOEDKOOP, Jerome GUINEE, Reinout HEIJUNGS, Mark HUIJBREGTS, Olivier JOLLIET, Manuele MARGNI, and SCHRYVER An DE. «Recommendations for Life Cycle Impact Assessment in the European context - based on existing environmental impact assessment models and factors (International Reference Life Cycle Data System - ILCD handbook)». In: (2011), p. 143. ISSN: 1018-5593. DOI: 10.2788/33030.

URL: https://publications.jrc.ec.europa.eu/repository/handle/JRC61049 (cit. on p. 28).

[85] Lidija Čuček, Jiří Jaromír Klemeš, and Zdravko Kravanja. «Overview of environmental footprints». In: *Assessing and Measuring Environmental Impact and Sustainability* (Jan. 2015), pp. 131–193. DOI: 10.1016/B978-0-12-799968-5.00005-1 (cit. on p. 29).

[86] *Database - ecoinvent*. URL: https://ecoinvent.org/database/ (cit. on p. 29).

[87] *ecoinvent v3.11 - ecoinvent*. URL: https://ecoinvent.org/ecoinvent-v3-11/ (cit. on pp. 29, 30).

[88] *openLCA.org*. URL: https://www.openlca.org/download/ (cit. on p. 29).

[89] Muhammad Aizaz Ud Din, Chuan Li, Lihan Zhang, Cuiping Han, and Baohua Li. «Recent progress and challenges on the bismuth-based anode for sodium-ion batteries and potassium-ion batteries». In: *Materials Today Physics* 21 (Nov. 2021), p. 100486. ISSN: 2542-5293. DOI: 10.1016/J.MTPHYS.2021.100486. URL: https://www.sciencedirect.com/science/article/pii/S2542529321001474 (cit. on p. 37).

[90] Seung Min Oh, Seung Taek Myung, Chong Seung Yoon, Jun Lu, Jusef Hassoun, Bruno Scrosati, Khalil Amine, and Yang Kook Sun. «Advanced Na[Ni0.25Fe0.5Mn0.25]O 2/C-Fe3O4 sodium-ion batteries using EMS electrolyte for energy storage». In: *Nano Letters* 14.3 (Mar. 2014), pp. 1620–1626. ISSN: 15306992. DOI: 10.1021/NL500077V (cit. on p. 37).

[91] *Altris 2.0*. URL: https://www.altris.se/news/altris-and-stora-enso-in-partnership-to-develop-hard-carbon-anode-material-for-sodium-ion-batteries (cit. on p. 37).

[92] Tanya Dagar, Rajkamal Arya, Ankush Kumar Singh, and Anil Kumar Sinha. «Advances in inorganic anode materials and progress in sodium-ion batteries: a comprehensive review». In: *Journal of Power Sources* 655 (Nov. 2025), p. 237945. ISSN: 0378-7753. DOI: 10.1016/J.JPOWSOUR.2025.237945. URL: https://www.sciencedirect.com/science/article/pii/S0378775325017811?dgcid=rss_sd_all (cit. on p. 37).

[93] Lingbing Ran, Ian Gentle, Tongen Lin, Bin Luo, Ning Mo, Masud Rana, Ming Li, Lianzhou Wang, and Ruth Knibbe. «Sn4P3@Porous carbon nanofiber as a self-supported anode for sodium-ion batteries». In: *Journal of Power Sources* 461 (June 2020), p. 228116. ISSN: 0378-7753. DOI: 10.1016/J.JPOWSOUR.2020.228116. URL: https://www.sciencedirect.com/science/article/pii/S0378775320304195 (cit. on p. 37).